TOMSK POLYTECHNIC UNIVERSITY ТОМСКИЙ ПОЛИТЕХНИЧЕСКИЙ УНИВЕРСИТЕТ

Министерство науки и высшего образования Российской Федерации
федеральное государственное автономное
образовательное учреждение высшего образования
«Национальный исследовательский Томский политехнический университет» (ТПУ)

Инженерная школа ядерных технологий
Направление подготовки 14.04.02 Ядерные физика и технологии
Отделение ядерно-топливного цикла

МАГИСТЕРСКАЯ ДИССЕРТАЦИЯ

Тема работы
Гибридная визуализация для планирования лучевой терапии опухолей головного мозга

УДК 615.849:616.831

Студент

Группа	ФИО	Подпись	Дата
0АМ0М	Атегека Мутамби		

Руководитель ВКР

Должность	ФИО	Ученая степень, звание	Подпись	Дата
Доцент ОЯТЦ ИЯТШ	Милойчикова Ирина Алексеевна	к.ф-м.н.		

КОНСУЛЬТАНТЫ ПО РАЗДЕЛАМ:

По разделу «Финансовый менеджмент, ресурсоэффективность и ресурсосбережение»

Должность	ФИО	Ученая степень, звание	Подпись	Дата
Доцент ОСГН ШИП	Спицына Любовь Юрьевна.	к.э.н.		

По разделу «Социальная ответственность»

Должность	ФИО	Ученая степень, звание	Подпись	Дата
Доцент ОЯТЦ ИЯТШ	Передерин Юрий Владимирович	к.т.н		

ДОПУСТИТЬ К ЗАЩИТЕ:

Руководитель ООП	ФИО	Ученая степень, звание	Подпись	Дата
Ядерная медицина	Верхотурова Вера Викторовна	к.и.н.		

Томск – 2022 г.

TOMSK POLYTECHNIC UNIVERSITY ТОМСКИЙ ПОЛИТЕХНИЧЕСКИЙ УНИВЕРСИТЕТ

Министерство науки и высшего образования Российской Федерации
федеральное государственное автономное
образовательное учреждение высшего образования
«Национальный исследовательский Томский политехнический университет» (ТПУ)

School of Nuclear Science & Engineering
Field of training: 14.04.02 Nuclear Science and Technology
Specialization: Nuclear medicine
Nuclear Fuel Cycle Division

MASTER THESIS

Topic of research work
Multimodality imaging application in Brain tumor Radiation therapy.

UDC 615.849:616.831

Student

Group	**Full name**	**Signature**	**Date**
0AM0M	Ategyeka Mutambi		

Scientific supervisor

Position	**Full name**	**Academic degree, academic rank**	**Signature**	**Date**
Associate Professor	Irina A. Miloichikova	Ph.D		

ADVISERS:

Section “Financial Management, Resource Efficiency and Resource Saving”

Position	**Full name**	**Academic degree, academic rank**	**Signature**	**Date**
Associate Professor	Luibov Y. Spicyna	Ph.D		

Section “Social Responsibility”

Position	**Full name**	**Academic degree, academic rank**	**Signature**	**Date**
Associate Professor	Yuriy V. Perederin	Ph.D		

ADMITTED TO DEFENSE:

Programme Director	**Full name**	**Academic degree, academic rank**	**Signature**	**Date**
Nuclear medicine	Vera V. Verkhoturova	Ph.D		

Tomsk – 2022

LEARNING OUTCOMES

Competence code	Competence name
Universal competences	
UC(U)-1	Ability to make critical analysis of problem-based situations using the systems analysis approach, and generate decisions and action plans.
UC(U)-2	Ability to run a project at all life-cycle stages.
UC(U)-3	Ability to organize and lead the teamwork and generate a team strategy to achieve the target goal.
UC(U)-4	Ability to use modern communication technologies to realize academic and professional interaction.
UC(U)-5	Ability to analyze and account for cultural diversity in the process of intercultural interaction.
UC(U)-6	Ability to set and pursue individual and professional activity priorities and ways to modify professional activity based on the self-esteem.
General professional competences	
GPC(U)-1	Ability to formulate goals and objectives of the research study, select assessment criteria, identify priorities for solving problems.
GPC(U)-2	Ability to apply modern research methods, evaluate and present the results of the performed research.
GPC(U)-3	Ability to present research outcomes in the form of articles, reports, scientific reports and presentations using computer layout systems and office software packages.
Professional competences	
PC(U)-1	Ability to maintain medical and technical documentation related to medico-physical aspects of radiation therapy, interventional radiology and radionuclide diagnostics and therapy.
PC(U)-2	Ability to ensure radiation safety of personnel, public, and the environment, to carry out monitoring of radiation exposure levels of patients, personnel, public, and the environment.
PC(U)-3	Ability to operate and maintain equipment and tools applied for the medical use of radiation.
PC(U)-4	Ability to manage the quality of physical and technical aspects within radiation therapy, diagnostics, interventional radiology and radionuclide diagnostics and therapy departments in accordance with the specific equipment requirements, regulatory requirements and staffing of a medical organization.
PC(U)-5	Ability to conduct and organize dosimetry planning, clinical dosimetry, quality assurance procedures for radiotherapy, interventional radiology, and radionuclide diagnostics and therapy.
PC(U)-6	Ability to apply knowledge of natural sciences, fundamental laws in the field of nuclear physics and technology, clinical and radiation standards, hygienic measures in nuclear medicine, which is sufficient to study issues associated with medical physics using modern equipment and information technology relying on the latest Russian and international experience.
PC(U)-7	Ability to develop reference books, tables and software containing data for clinical use in dosimetric planning of radiation therapy, radionuclide diagnostics and therapy.
PC(U)-8	Ability to take part in the design and physical and technical equipment development for radiation therapy, diagnostics, interventional radiology

	and radionuclide diagnostics and therapy, and radiation safety divisions.
PC(U)-9	Ability to conduct training sessions and develop instructional materials for the training courses within the cycle of professional training programs (bachelor degree programs).

TOMSK POLYTECHNIC UNIVERSITY ТОМСКИЙ ПОЛИТЕХНИЧЕСКИЙ УНИВЕРСИТЕТ

Министерство науки и высшего образования Российской Федерации
федеральное государственное автономное
образовательное учреждение высшего образования
«Национальный исследовательский Томский политехнический университет» (ТПУ)

School of Nuclear Science & Engineering
Field of training (specialty): 14.04.02 Nuclear Science and Technology
Specialization: Nuclear medicine
Level of education: Master degree program
Nuclear Fuel Cycle Division
Period of completion: 2020/2021and 2021/2022 academic years

Form of presenting the work:

Master Thesis

SCHEDULED ASSESSMENT CALENDAR
for the Master Thesis completion

Deadline for completion of Master's Graduation Thesis:	06.06.2022

Assessment date	Title of section (module) / type of work (research)	Maximum score for the section (module)
27.01.2022	Preparation of technical specifications and selection of research areas	10
24.02.2022	Development of a common research methodology	10
23.03.2022	Selection and study of materials on the topic	10
13.04.2022	Experimental research	20
27.04.2022	Processing received data	20
18.05.2022	Registration of the work performed	15
30.05.2022	Preparation for defending a dissertation	15

COMPILED BY:
Scientific supervisor:

Position	Full name	Academic degree, academic status	Signature	Date
Associate Professor	Irina A. Miloichikova	Ph.D.		

APPROVED BY:

Program Director	Full name	Academic degree, academic status	Signature	Date
Nuclear medicine	Vera V. Verkhoturova	Ph.D		

TASK FOR CHAPTER
«FINANCIAL MANAGEMENT, RESOURCE EFFICIENCY AND RESOURCE SAVING»

Student:

Group	Name
0AM0M	Ategyeka Mutambi

School	School of nuclear technology engineering	School division	Division of Nuclear Fuel Cycle
Level of qualification	Master degree	Field of study	14.04.02 Nuclear Physics and Technology

Initial data for chapter «Financial management, resource efficiency and resource saving»:	
• *The cost of scientific research resources: material, technical, energy, financial, informational and human*	*Project budget **518890** rubles:* *The cost of purchasing equipment – 53 thousand rubles, the cost of a salary for a supervisor –123 thousand rubles, etc.*
• *The system of taxation used, tax rates, volumes of payments, discounts and loans*	*According to clause 3 of subclause 16 of Art. 149 of the Tax Code of the Russian Federation, this project is not subject to taxation. Based on Chapter 34 of the Tax Code of the Russian Federation, since 2016, the rate of 30.2% of the wage fund has been used to calculate contributions to extra-budgetary funds.*
Problems to research, calculate and describe:	
• Project initiation	Project goals and results, project structure, assumptions and limitations, planning, budgeting, etc.
• Economic model development	Calculation of initial investment, calculation of funds obtained from fuel savings, calculation of cash flows over 20 years
• Determining the effectiveness of projects	Net Present Value Calculation and Sensitivity Analysis
• Final decision making	Selecting and evaluating criteria, weighing the criteria and calculating the most appropriate solution
Graphic materials:	
1. Competitive power of the project *2. SWOT matrix* *3. Stakeholders of the project* *4. Project goals and results* *5. Project working group* *6. Limitations and assumptions* *7. Assessment of the prospects of a new product* *8. Plan of investments. The budget for scientific and technical research*	

Assignment date	

Consultant:

Position	Name	Academic degree	Signature	Date
Associate Professor	Luibov Y. Spicyna	Ph.D		

Student:

Group	Name	Signature	Date
0AM0M	Ategyeka Mutambi		

TASK FOR SECTION
«SOCIAL RESPONSIBILITY»

For a student:

Group	Name
0AM0M	Ategyeka Mutambi

School	School of nuclear technology engineering	School division	Division of Nuclear Fuel Cycle
Level of qualification	Master degree	Field of study	14.04.02 Nuclear Physics and Technology

Topic of research work:

Multimodality imaging application in Brain tumor Radiation therapy.	
Initial data for section «Social Responsibility»:	
1. Information about object of investigation (matter, material, device, algorithm, procedure, workplace) and area of its application	*The object of investigation is multimodality imaging application in Brain tumor Radiation therapy planning.* *The applications and limitations of different imaging modalities under study will be analysed and recommendations given, which may be useful for oncology institutions and hospitals.*
List of items to be investigated and to be developed:	
1. Legal and organizational issues to provide safety: – Special (specific for operation of objects of investigation, designed workplace) legal rules of labor legislation; – Organizational activities for layout of workplace.	– Labour code of Russian Federation #197 from 30/12/2001 GOST 12.2.032-78 SSBT – Sanitary Rules 2.2.2/2.4.1340-03. Hygienic requirements for PC and work with it
2. Work Safety: 2.1. Analysis of identified harmful and dangerous factors 2.2. Justification of measures to reduce probability of harmful and dangerous factors	– Enhanced electromagnetic radiation level – Insufficient illumination of workplace – Excessive noise – Deviation of microclimate indicators – Electric shock
3. Ecological safety:	– Indicate impact of MRI, CT and SPECT machines on hydrosphere, atmosphere and lithosphere
4. Safety in emergency situations:	– Fire safety;

Date of issuance of the task for the section according to the schedule	

The task was issued by adviser:

Position	Full name	Academic degree, academic rank	Signature	Date
Associate Professor	Yuriy V. Perederin	Ph.D		

The task was accepted by the student:

Group	Full name	Signature	Date
0AM0M	Ategyeka Mutambi		

Table of acronyms.

SPECT	Single Photon Emission Tomography
PET	Positron Emission Tomography
CT	Computed Tomography
MRI	Magnetic Resonance Imaging
RTP	Radiotherapy Planning
CNS	Central Nervous System
WHO	World Health Organization
IMRT	Intensity Modulated Radiation Therapy
3D-CRT	3-D Conventional radiation therapy
NMR	Nuclear Magnetic Resonance
FOV	Field of View
MP-RAGE	magnetization-prepared rapid gradient-echo
T2 SPACE	T2 sampling perfection with application-optimized contrasts
EORTC	European Organization for Research and Treatment of Cancer
RTOG	Radiation Therapy Oncology Group
GTV	Gross tumor volume
CTV	Clinical target volume
PTV	Planning target volume
MIBI	methoxyisobutylisonitrile
ACNS	American Clinical Neurophysiology Society
DICOM	Digital Imaging and Communications in Medicine

Contents

1 Multimodality imaging for brain tumor radiation therapy.

Brain tumors are masses of abnormal uncontrolled cell growth in the brain. Whereas in other parts of the body, we are interested in distinguishing between benign, that is non-cancerous and malignant that is cancerous tumors, especially since benign tumors neither grow into nearby tissues nor spread to distant areas and are almost never life-threatening while malignant tumors are so dangerous because they can spread throughout the body, brain tumors whether malignant or otherwise can be life threatening.

1.1 Demography of brain tumors.

The incidence rate of newly diagnosed primary malignant brain tumors is estimated at 3.8 every 100,000 males and 3.1 every 100,000 females annually. This rate is higher in developed countries (males: 5.8 per 100,000; females: 4.4 per 100,000) than in less developed countries (males: 3.2 per 100,000; females: 2.8 per 100,000). About 70 % of these tumors are GBM, 10–15 % AA, 10 % AO and AOA and the rest are less common tumor entities like ependymomas and anaplastic gangliogliomas [4, 5]. Due to the improvement in diagnostic abilities, there has been a rise in the CNS tumor incidence rates in the recent years, [6] as seen in the trend graph in figure 1-1.

From the American Cancer Society estimates, about 24,530 malignant tumors of the brain or spinal cord (13,840 in males and 10,690 in females) will be diagnosed in 2022. These numbers would be much higher if benign (non-cancer) tumors were also included.

About 18,600 people (10,500 males and 8,100 females) will die from brain and spinal cord tumors.

Overall, the chance that a person will develop a malignant tumor of the brain or spinal cord in his or her lifetime is less than 1%. The risk of developing any type of brain or spinal cord tumor is slightly higher among women than among men, although the risk of developing a malignant tumor is slightly higher for men than for women.

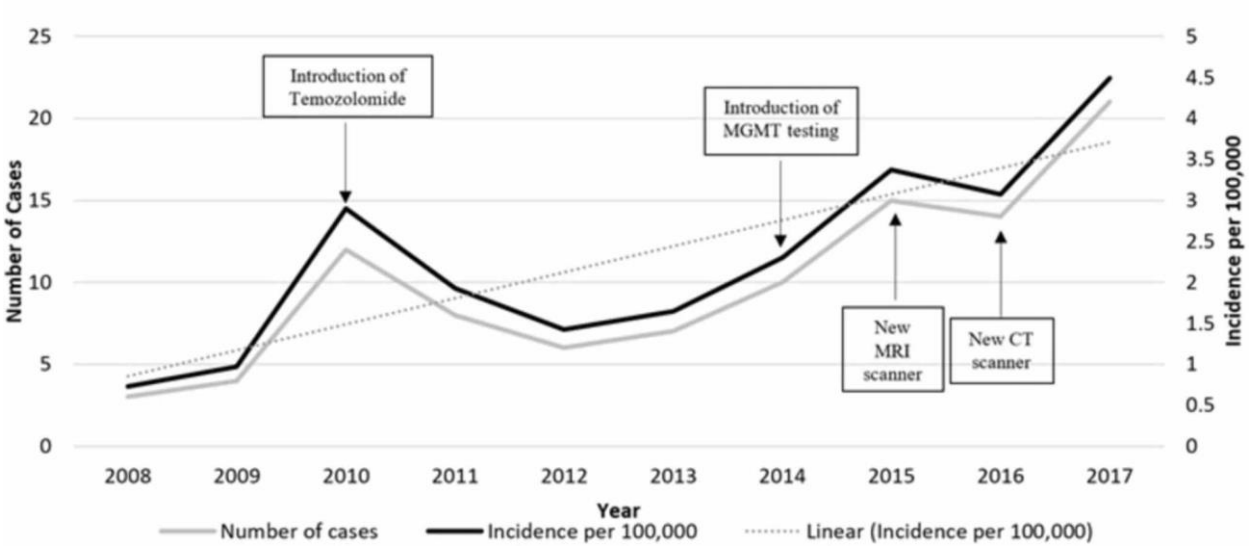

Figure 1-1 Trends in incidence rates of CNS tumors [6].

1.2 Brain tumor classification.

CNS tumor histological classification is not fully agreed on and we see it constantly updating as more is discovered about the tumors. For example, the WHO classification has been updated five times, with the latest update being in 2021. [7] [8] Six different histopathological groups are recognized, according to the type of cells from which they originate:

- Neoplasm arising from peripheral nerves but in rare cases appear in the brain. Neuroblastomas show rapid growth and are seen more in children.
- Neuroepithelial tissue tumors, including astrocytomas and oligodendrogliomas are the most common among the primary tumors.
- Neoplasms from meninges, which mainly include meningiomas, are usually slow progressing. Meningiomas, the commonest benign brain tumor in adults, are usually treated by surgery or radiotherapy.
- Hematopoietic and lymphatic tissue neoplasms including hemangioblastomas, hemangiopericytomas primary CNS lymphomas are common and surgery and radiotherapy play a big role in management.

- Germ cell tumors have different types, including germonomas, which are the most common type. They are more common in younger ages.
- Neoplasms from the sellar region are considered separately, and include pituitary adenomas, and Rathke's cleft cyst, whose cells originate from the nasal area, and can also be treated with radiosurgery.

The primary brain tumors from the neuroepithelial tissue are the commonest that is gliomas, which derive from glial cells, representing approximately 45% of all primary brain tumors and are highly malignant as seen in figure 1-2. Gliomas are sub-classified into astrocytic, that is, astrocytoma, oligodendroglial, ependymal, or mixed tumors. Astrocytomas are further subdivided into four grades of severity in relation to their histopahological features, including grade I for low grade, grade II for high grade, grade III for anaplastic astrocytomas, and grade IV for glioblastoma multiforme.

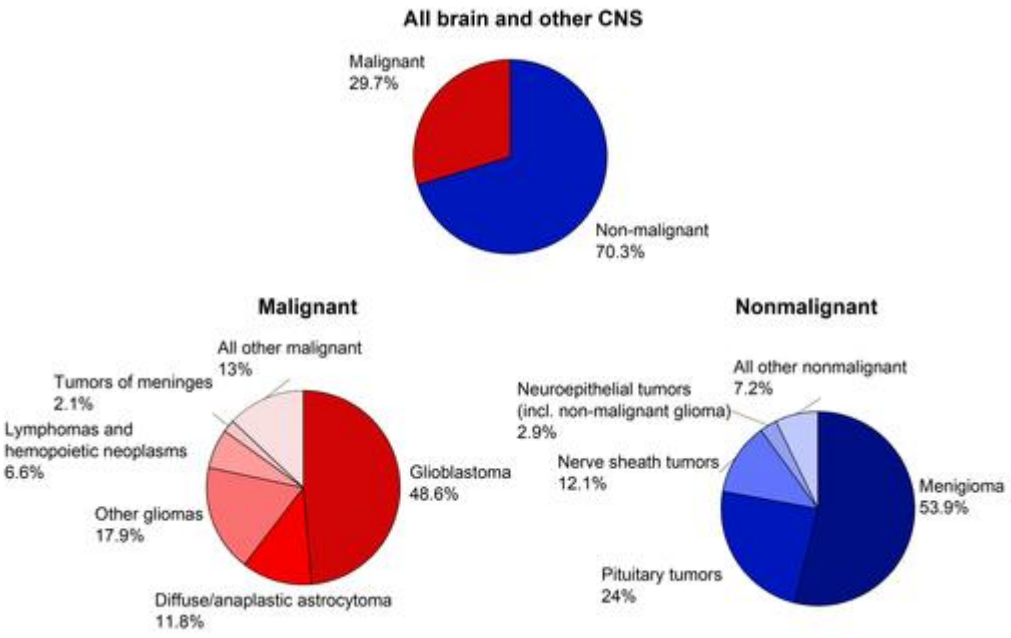

Figure 1-2 Brain tumors by histological types and malignancy. [9]

Brain tumors rarely spread to other parts of the body, but most of them can spread through the brain tissue.

The grading system widely considered to choose treatment for gliomas is the WHO grading system which has grades from 1 to 4, with grade 1 as the least aggressive then grade 4 as the most aggressive. This classification considers 5

histopathology criteria in accordance with the extent of anaplasia, including nuclear atypia, cellular density, endothelial proliferation, mitosis, and necrosis. Below are the features considered for each WHO malignant grade:

- WHO Grade II: has moderately increased cellular density, and occasionally may have nuclear atypia, but no or a maximum one mitosis, with no necrosis or endothelial proliferation.
- WHO Grade III: has increased cellular density, nuclear atypia is distinct, with marked mitotic activity, but no necrosis and no endothelial proliferation.
- WHO Grade IV: has a high cellular density, marked nuclear atypia, the mitotic activity is high, and there is marked necrosis and endothelial proliferation.

1.3 Brain tumor management approaches.

The treatment approach varies depending on the WHO grade and the histological type. The options include surgical resection, radiotherapy, chemotherapy, targeted drug therapy and electric field therapy. Usually either one or a combination of these approaches is used. The commonly used approach is surgical resection to remove most of the tumor followed by chemotherapy or radiotherapy to kill the remaining tumor cells.

1.3.1 Surgery.

Surgery has two roles, the first being to get tissue for histological analysis and to completely or partially remove the tumor volume, hence relieving pressure to the surrounding brain tissue.

After the investigations and clinical assessment show that it is a low-grade glioma, a decision has to be made, on whether it is resectable or not resectable. This decision is made considering different factors, like patient age, tumor size, shape, number of lesions, their location and the histological nature of the tumor. For surgical patients, a decision has to be made on the surgical approach to use. The different

approaches include gross total resection, MRI guided laser interstitial thermal therapy, open biopsy and debulking, thermotherapy implants if indicated.

Following complete resection, no treatment will be required in some cases like pilocytic astrocytoma or pleomorphic xanthoastrocytoma. However, most cases will require follow up treatment just as done in incomplete resection. This will include radiotherapy and/or chemotherapy.

MRI is recommended at least 48 hours after surgical resection to know the extent of the resection then a follow up MRI every 3 to 6 months for 3 to 5 years and then once a year as clinically needed.

1.3.2 Chemotherapy

One or a combination of drugs can be used in glioma treatment. Temozolomide is the chemotherapy drug commonly used for glioma treatment singly but a PCV (procarbazine, lomustine and vincristine) combination can also be used. Platinum based combinations including cisplatin and carboplatin are mostly used for relapse cases. Other options include carmustine wafers, regorafenib and etoposide.

Chemotherapy for gliomas is mostly given in combination with radiotherapy, and this can be at the same time, that is concurrent treatment, after radiotherapy as adjuvant treatment or both. Treatment is given in cycles with periods of recovery in between for the normal body cells to recover before the next cycle is given.

1.3.3 Radiation therapy

Radiation therapy is used in brain tumors after total or partial resection to destroy the remaining tumor cells or in palliative care to reduce the mass effects of the tumor. There are different methods of delivering radiotherapy for brain tumors depending on the type of tumor, site and the goal of treatment. These include

- External beam radiation therapy, which is the commonest and in which the treatment machine moves around the patient delivering treatment from a distance from the patient. The size and shape of the beam and the dose are controlled on a computer treatment system. The two types of EBRT used for brain tumors are 3-D CRT and IMRT.

- 3-D CRT uses the data from imaging to create a 3-D model of the tumor and beams are made from different angles to target the tumor and reduce the dose to the normal brain tissue. IMRT delivers the dose more precisely to the tumor because the beams are divided into several beamlets and at many different angles and the intensity of each beam is modulated to give a more precise dose distribution.
- Stereotactic radiosurgery (SRS) is a form of radiotherapy where very high doses are delivered to a small area using machines like a gamma knife or a Cyberknife in a few (usually less than 5) fractions. This treatment is a priority for treating tumors in hard to reach areas or in patients who are not fit for surgery.

1.4 Imaging modalities for radiotherapy planning.

Medical imaging in radiotherapy planning plays a very vital role since it determines the accuracy in dose delivery to the tumor tissue, hence sparing the normal surrounding tissues. This is the main Goal in radiation therapy. There is no single imaging modality that meets all the Radiotherapy requirements. The different imaging modalities available play different roles, and offer different advantages.

1.4.1 Computed tomography.

Computed tomography (CT) imaging has long been the standard of care for imaging to plan radiation therapy (RT) treatments [9]. After its clinical introduction in 1971, computed tomography (CT) has improved from an X-ray modality that was limited to axial imaging of the brain in neuro-radiology into a 3-D whole body imaging modality for a wide range of applications, including oncology, vascular radiology, cardiology, traumatology and interventional radiology. CT is applied for diagnosis and follow-up studies of patients, for planning of radiotherapy, and even for screening of healthy subpopulations with specific risk factors.

CT offers several clinical advantages for treatment planning, including direct measurement of electron densities for radiation dose calculations. This gives it an advantage over other modalities in treatment planning. Clear visualization of high

contrast bony landmarks due to the higher linear attenuation values for the bone; which can even be made better by using ultrahigh-resolution CT (U-HRCT) that provides better spatial resolution than conventional multi-detector row CT (ConvCT) using smaller collimation, more channels and detector rows, smaller focus size, and allows a higher matrix display.

Numerous measurements of x-ray transmissions through the body are used to reconstruct a CT image. Prior to image reconstruction, a logarithm of the measured data is calculated.

The intensity of x-rays after passing through a particular part of the object is given by the Lambert-Beer law:

$$I(d) = I_0 e^{\mu x} \tag{1.1}$$

where, I_0 is the intensity of x-rays before the object, I(d) is intensity of the attenuated beam, μ is the linear attenuation coefficient, x is the thickness of the material. The sum of the linear attenuation coefficients along the line can be estimated by computing the projection value:

$$p = -\ln\left[\frac{N(E)}{N_0(E)}\right] = \int_l \mu\,(s, E)\,ds \tag{1.2}$$

In planar x-ray imaging, projection values are what you see in the image and a projection with high attenuation (e.g. bone) is represented with lighter color, and a point of low attenuation (e.g. air) is represented with a darker color. Since each point in a planar x-ray image represents the sum of the attenuation on the line between the source and the detector, the image will consist of the superposition of all the internal structures in the object. In many medical situations, specifically when imaging small and low contrast objects, planar x-ray images are not sufficient to make a diagnosis. The solution comes with x-ray computed tomography, or more commonly, CT. The basic idea of CT is to acquire images of the patient from many different angles and then mathematically reconstruct the interior composition of the object. The result is that the x-ray attenuation can be estimated for each separate point in the patient. The 3-dimensional image data is generally visualized by presenting different slices

through the object. Each individual slice will not contain any overlapping structures, making also small and low-contrast objects detectable.

Mathematically, computed tomography is based on the Radon transform, which was introduced by Johann Radon in 1917. The 2D Radon transform is an integral transform that can be expressed

$$R[f(x,y)](r,\theta) = \int_{(x,y;r,\theta)} f(x,y)dxdy \tag{1.3}$$

$$\text{where}(x,y;r,\theta) = \{x,y|x\cos\theta + y\sin\theta = r\} \tag{1.4}$$

The left side of Figure 1-3 shows how r and θ define a projection line. An image of the 2D Radon transform of an object is referred to as a sinogram since points in the object are represented by sinusoidal waves in the 2D Radon transform. Having acquired the measurements of the projection values for all r and θ, we can reconstruct a map over the distribution of the attenuation coefficient in the interior of the object.

If we acquire the projections on a Cartesian grid in θ and r, then we have sampled the 2D Fourier transform of the object on a polar grid in u and v. The original object can therefore be retrieved by performing an inverse 2D Fourier transform in polar coordinates:

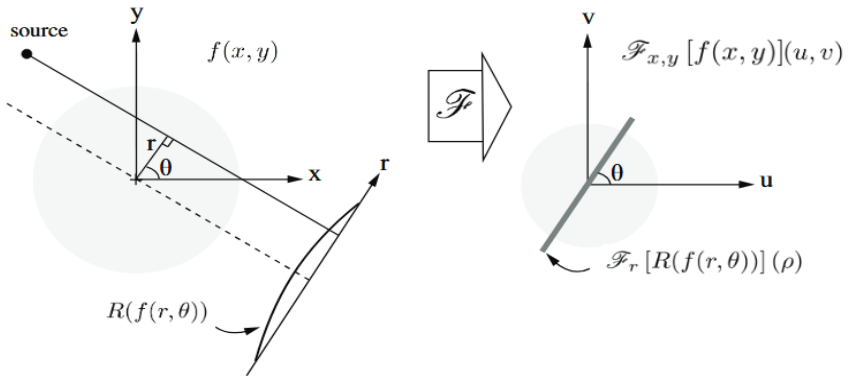

Figure 1-3 An illustration of the projection-slice theorem. [10]

To the left is the original object and to the right is the 2D Fourier transform of the object. By Acquiring projection measurements $R[f(x,y)](r,\theta)$ at many angles one can build up the 2D Fourier transform of the object $F_{x,y}[f(x,y)](u,v)$. The original object can then be retrieved by an inverse Fourier transform.

Filtered back projection (FBP) is the most commonly used method for CT image reconstruction.

$F_r[R[f(x,y)](r,\theta)]$ (ρ), are filtered by a ramp filter, $|\rho|$. Then the filtered signal is 1D inverse Fourier transformed with respect to ρ, and finally the signal is back projected (values are assigned to the points(x,y)on the lines $x\cos\theta+y\sin\theta=$constant) and summed for all angles. It is worth noticing that it is only necessary to acquire data for $\theta \in [0,180^o)$.

We have seen that if we can estimate the 2D Radon transform of an object, then we can estimate inner structures of the object using filtered back projection. We get the object's 2D Radon transform by measuring the x-ray transmission through the object for a large number of angles, and preferably very fast. In the first CT systems, the image was acquired using a pencil beam that was stepped and rotated [10].

In modern medical CT systems, the images are acquired using a point source, (x-ray tube) and a large opposing detector that measures the transmitted x-rays. This geometry is referred to as fan-beam CT. The projections in fan-beam CT are generally described by the coordinates β and γ, where β is the angular position of a projection in the fan ($\beta= 0$ applies to the beam that passes through the center of rotation) and γ is the angular position of the source. The definitions of β and γ are given in Figure 1-4

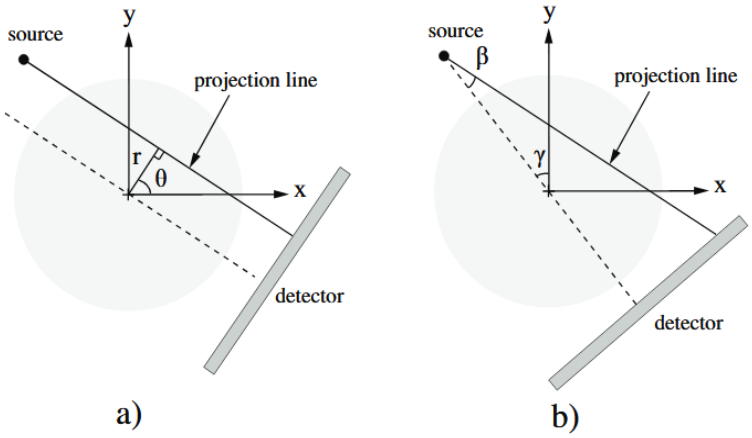

Figure 1-4 The definitions of β and γ in fan beam geometry [10].

The definitions of a) r and θ describing the projection lines in parallel-beam geometry and b) γ and β describing the projections in fan-beam geometry. Both the detector and the source are mounted on a gantry that rotates continuously around the patient. The detector is digital (meaning that, in the end, the output value is ones and zeros) and the detector elements are referred to as pixels (not to be confused with the pixels of the reconstructed image). If the detector is extended also along the axis of rotation (also known as the axial direction) the geometry is referred to as cone beam CT. And if the patient table is moved continuously in the axial direction during the image acquisition, the geometry is referred to as helical, or spiral CT.

The center of rotation is commonly referred to as the isocenter, the set of projections measured at a certain angle is often referred to as a view and the time during which a single measurement is acquired is referred to as the frame time.

Clear visualization of bony landmarks is very important because of the effect of bone on the treatment beams [11]. Other advantages that make it the standard for treatment and dosimetric planning are excellent spatial fidelity with no distortion of anatomy compared to MRI, [12] and the ability to display some soft tissue contrast for delineation.

Despite being the standard of care, CT imaging for radiotherapy planning offers its own set of challenges, not the least of which is it delivers extra radiation dose outside the target treatment area, and potential image artifacts.

Causes and Types of CT Image Artifacts

Imaging artifacts arise when there is a systematic difference between the reconstructed CT numbers and the true attenuation coefficients of the tissues being imaged. This results in part of the image being distorted or obscured.

CT scans can be impacted by a variety of image artifacts, including ring artifacts caused by miscalibration of the scanner or failure of the detector element, cupping caused when polychromatic X-rays traverse through the body and become hardened, or a differential attenuation in the image. Streaking or banding is another form which is typically caused by bony anatomy and/or wide patient posture then motion artifacts caused by voluntary or involuntary movement of the patient during the scan and metal artifacts caused when the area being imaged has or is adjacent to a metallic object (implanted or external). The beam attenuation through the metal is not well approximated; this results in streaking, beam hardening or even a loss of information where the metal and tissue interface [13].

The metal artifact effect is reduced using different metal artifact reduction algorithms. [14]

Due to organ movement, especially lungs and heart there is a challenge in estimating the tumor size and position at different stations of the breathing cycle while using 3D CT. This organ movement affects mainly the chest and the abdominal organs due to the movement of the diaphragm. This gives us images with a mismatch in the tumor location and size according to which part of the cycle of respiration the image is taken [15]. Four-dimensional (4D)-CT scan is one of the approaches that reduces motion induced tumor mismatches. 4D-CT scanning is defined as CT acquisition at a respiratory time scale so as to capture the shape and trajectory of moving organs during breathing. [16] Other approaches to tackle organ movement include breath holding, gated CT and slow CT. Another new technology that solves this problem is the MRI guided radiotherapy, where the MRI is built in the treatment system and real time images are used to deliver treatment to only the cancer tissue [17].

1.4.2 Magnetic resonance imaging.

Although in many cases CT still acts as the master reference scan, MRI provides superior soft tissue contrast compared to CT, as well as a myriad of information on tumor characteristics that aid the delineation of both the tumor and organs at risk. The flexibility to acquire multiple contrasts has shown advantages for accurate tumor delineation in a large body of literature over the recent years [18].

MRI is a gold standard for visualization of brain tumors. It is also routinely utilized in some tumors for treatment planning [19]. T_2 weighted imaging, for example, is able to distinguish tumor from normal tissue and fat in rectal and esophageal cancer, whereas T_1 weighted imaging provides good tumor contrast in squamous cell carcinoma in neck and head cancer [20].

Magnetic resonance image acquisition.

In MR imaging, we take advantage of the spin property of the hydrogen one nucleus. The proton in the hydrogen nucleus being positively charged has a magnetic moment because it is constantly spinning. This exam is done by applying a magnetic field and radiofrequency waves to the body. Currently most machines used have magnets with 1.5 or 3 T. Commercial systems at much higher magnetic fields (such as 7 T) are also now available. While these give increased signal-to-noise ratios for all types of MRI they still face many technical challenges, such as a limited range of signal detection coils, and high radio-frequency power deposition, and therefore are currently primarily used in research Institutions. Other nuclei possess the spin property but they are not as abundant as hydrogen in the human body. These include 31P, 23Na, 13C

but they are applied in NMR spectroscopy not much in clinical imaging.

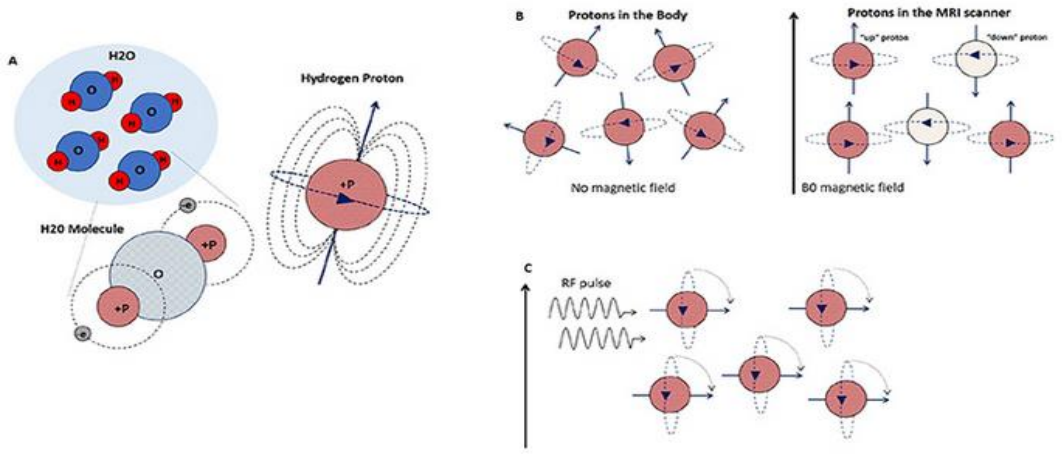

Figure 1-5 Illustrating the principle of MRI [21].

In absence of an external magnetic field, protons are arranged in a random manner and have a net magnetization vector of zero. When we apply the magnetic field, they will all align parallel to it. We have more than half of them process in the direction of the magnetic field(B0) and the less fraction in the direction against the magnetic field, creating a small net magnetization vector. Those against the main magnetic field are in a high energy state, and the others are in a lower energy state. Then a radiofrequency (RF) pulse is applied, causing the rotation of the net magnetization vector to the transverse plane. After the RF pulse is removed, the energy is lost in the form of electromagnetic energy which is detected by radiofrequency coils in the scanner as the net magnetization vector caused by the RF pulse exponentially decays off as illustrated in figure 1-6. Different protons process differently according to the surrounding environment due to varying electron shielding from the energy given by the RF pulse. This gives us transverse relaxation, which is referred to as T2 relaxation. The other time measured is for the relaxation in relation to the main field. This is called longitudinal relaxation, or T1 relaxation, which is longer than t2. Both T1 and 2 for fluids are longer because the protons in fluids are less shielded and hence they take longer to lose their energy and hence longer relaxation time. Protons in highly shielded regions lose their energy faster and have lower relaxation time. This is why the fluids like cerebral spinal fluid appear bright on T2 images and darker on T1 images.

Besides native T_1 and T_2 contrast, physiological contrasts such as dynamic contrast enhanced (DCE), blood oxygen level dependent (BOLD), and diffusion weighted imaging (DWI) have been shown to have added value in defining tumor boundaries.

MRI uses non-ionizing radiation and this is a big advantage because it minimizes patients' radiation exposure. This makes it better for use in young chilPh.Den and in patients who need follow up imaging to help in case of need for treatment adjustment during treatment.

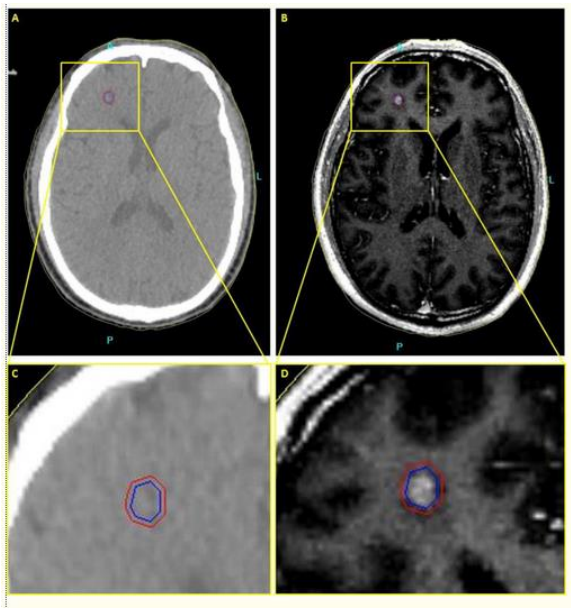

Figure 1-7 Axial brain images of a patient with a metastatic tumor in the brain [22].

From figure 1-6, for (A,C) CT image, no contrast between the tumor and the surrounding normal tissue. (B,D) T2-weighted Fluid-attenuated inversion recovery image (FLAIR) MR image. Higher soft tissue contrast of the MR image leads to more accurate delineation of the tumor [22].

There are different approaches to treatment of tumors affected by respiratory movement, which include breath holding, use of 4D CT use of the gating method. The other approach to this is real-time image guided radiotherapy, where they visualize the tumor in real time during treatment and deliver the radiation dose only when the tumor is in the planned treatment volume. LINACs built with MRI are already in use for this function in some centers [23].

CT scan gives us the mass attenuation coefficients of the tissue which is used to get the Hounsfield units in the material, which gives us information on the electron densities and hence helps in dose calculation. MRI images do not give us this important information and hence it has been hard to use MRI-alone treatment planning. The other way is to assign attenuation coefficients to different anatomical structures then make outlines on the different organs in the image and assign electron densities. The other approach is when we superimpose the MRI image on a CT scan and we use the electron density values from the CT image. In this way, we are able to take advantage of the good contrast from MRI and the dose calculations from the CT image [24].

Poor Cortical bone signal: MRI gives very low signal intensity from cortical bone. A good estimation of bone intensity and the extent of the bones, including their clear outlines is very important in dose calculation. At the points where bone interfaces with tissues or air we usually have beam scattering which will greatly affect the dose distribution.

Image distortions in MRI: Ideally, the magnetic field in the MRI system should be invariable. However, many systems in use have non-uniform magnetic fields. Radiofrequency field non-uniformities also reduce the accuracy of MR-based planning. This, among other factors like gradients being nonlinear, cause distortion of the geometry of the anatomy [25].

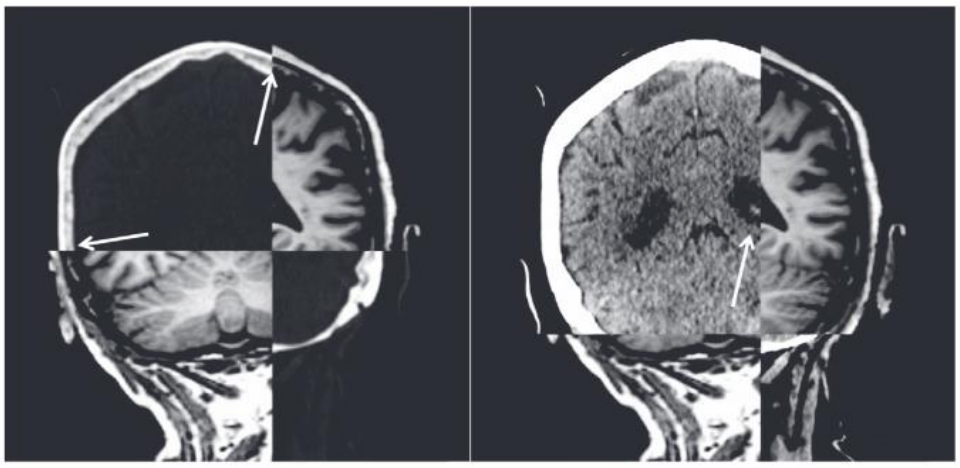

Figure 1-8 3D T1-weighted sequence of the brain registered to a planning CT. Modified from [26].

In Figure 1-7 we see a diagnostic 3D T1-weighted sequence of the brain with a water-fat shift of 2 pixels (size 11mm2), registered to a planning CT. Left: window-level of the CT scan set to show cortical bone and bone marrow. The cortical bone is bright on CT, dark on MRI (arrows). Right: window-level of the CT scan set to show the contrast in soft tissue in the brain. The registration of both MRI and CT is identical between left and right. The arrow points at the ventricle that appears shifted on MRI relative to CT.

1.4.3 Single Photon Emission Computed Tomography.

SPECT is a medical imaging modality that uses the emission tomography technique. A radioisotope is injected in the body and the amount of radiation measured in different regions of the body represents the function of tissues in that region. In SPECT, the radiotracer emits photons which are detected as independent events, unlike in PET imaging, which will be talked about in the next chapter. SPECT has widely been used in oncology, especially in cancer staging because its ability to detect metastasis to lymph nodes and in non-small cell lung cancer (NSCLC) using technetium 99m, the lung function is accessed which is considered in radiotherapy planning with the aim of saving the functional lung tissue.

The main advantage of the nuclear medicine medical imaging techniques (SPECT and PET) which are functional imaging modalities lies in their ability to give us information about the function of tissue in a certain body region, which often precedes the anatomical changes in the disease process [27].

Single-photon emission computed tomography image acquisition

For SPECT the first step is administration of a radiopharmaceutical, which may be injected, inhaled or ingested according to the type of radiopharmaceutical used. A delay time is given for the bio-distribution of the tracer in the body, after which the radiations emitted from the patient are detected and used to generate tomographic images. In SPECT, a gamma camera is used to detect photons emitted by the radiotracer.

Most gamma cameras used are made of sodium iodide scintillators because of their high light output and detection efficiency, good energy resolution and stopping power at expected energies, not forgetting that it's economical.

In front of the gamma camera we have a lead collimator. The properties of the collimator depend on the photons being targeted, and its resolution also depends on the distance from the patient. This is why the collimator is positioned as close to the patient as possible, which is done in consideration of the inverse square rule of the photon flux and the probability of crystal area detection to the distance. The collimator helps to remove the rays from other directions, so that only rays normal to the detector are detected.

To acquire a SPECT the gamma camera is rotated around the patient as data is acquired into the computer digital matrix at all the sampled angles.

Ideally in an imaging system, projections which are opposite to each other are considered to mirror each other. However, the gamma camera used in nuclear medicine imaging is not a perfect system, therefore, the views opposite to each other are not the same. This is firstly because, as the distance from the camera to the object being imaged increases, the resolution of the gamma camera reduces. Secondly, there is an acceptable Compton scatter percentage as photopeak gamma rays, because of the camera's finite energy resolution. Thirdly, some fraction of gamma rays from the object is attenuated since they are traveling in an attenuating medium, that is, the body of the patient. Therefore, in most SPECT studies, 360° of arc is made for a more accurate reconstruction. However, for myocardial imaging, 180° arc acquisition is used in practice.

In SPECT imaging the selection of the size of the matrix in the computer is a very important aspect in the projection views. Essentially, the field of view (FOV) of the gamma camera is divided into square areas (pixels) by the computer. The matrix size is chosen depending on several factors. Firstly, ideally the size of a pixel should, be less than a third of the expected full-width at half-maximum (FWHM) resolution of the system used, measured at the center of rotation specific for the isotope used, and not forgetting the radius of rotation (that is the distance of camera from patient)

and the effects of the collimator. The size of a pixel, D, in millimeters, may be calculated:

$$D = FOV / (Z \times n), \quad (1.5)$$

Where: FOV (mm) is the widest dimension of the computer image matrix

Z is the zoom factor during acquisition, which may be 1.5 or 2.

N is the number of pixels which can for example be 64 or 128.

Higher SPECT resolution requires the use of a smaller pixel size. However, smaller pixel sizes lead to increased noise hence poorer pixel signal-to-noise ratio.

Ideally, for accurate reconstruction the number of angular views in the 360° arc should at least be equal to the matrix size of the projection image. Streak artifacts are likely to appear during reconstruction, or even quality loss if the number of views is reduced below the minimum.

Then, during SPECT acquisition in practice, the camera moves in and out radially rotating around the patient, hence the name non-circular orbit (NCO). Some SPECT techniques may also be capable of acquiring data both using the standard step-and-shoot mode and the continuous mode. In the step-and-shoot mode there is an alternate rotating to the next view (step) and then the camera stops and acquires a projection (shoot). Acquiring 120 views over 360° is enough to make the blurring effect caused by delay during the camera rotation between the views insignificant.

Two-dimensional photographs of a three-dimensional scene, taken from different directions may be reconstructed in 3 dimensions. The projections have to be modified mathematically to accurately reconstruct the three-dimensional distribution. As seen in image below, using the gamma camera, the three-dimensional (x,y,z) object is viewed as layers of two-dimensional (x,y) slices of finite thickness dz stacked together. The volume elements (voxels), in each slice are projected onto the gamma camera as a horizontal row of picture elements (pixels) along X8, at a particular height along Y8. The approach of filtered back projection is based on the Radon transform, a mathematical theory used in image reconstruction from different projections.

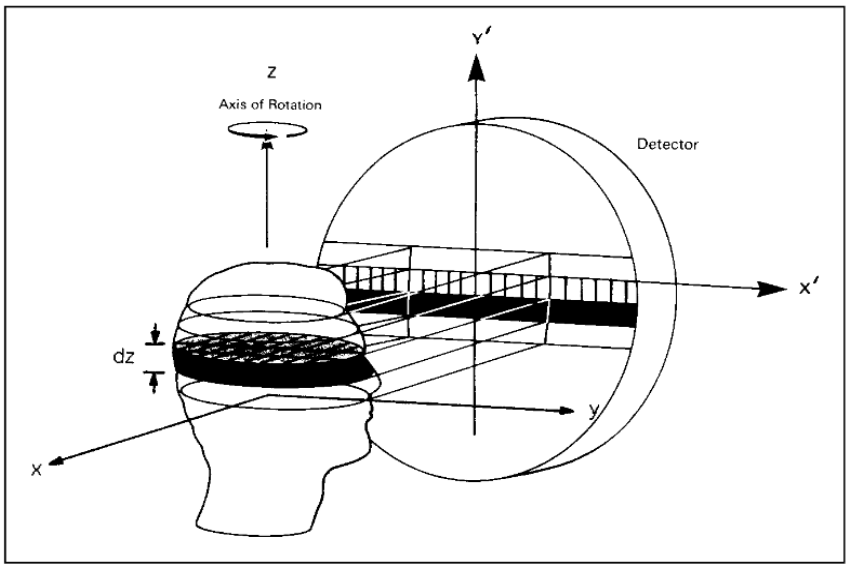

Figure 1-9 Diagram of SPECT projection imaging process (radon transform).

In filtered back projection reconstruction, each projection image row is viewed as the object's projection in one-dimensional representation. The profiles of the one-dimensional pixel may be modified mathematically or filtered. Then they are projected back across the two-dimensional slice at their respective angles (ergo back projection). Then the two-dimensional space back projections are added together to form the reconstructed transverse image in two-dimensional space.

In the iterative method of reconstruction, however, we have an estimate of the probability of a particular amount of radioactivity at a specified location being detected at a particular point in each projection by the imaging system. In the iterative model we put into consideration things like the physics phenomena, such as the system's spatial resolution which caters for the variation with distance from the collimator, attenuation e.g., from the transmission source scans, and also considers Compton scattering. Iterative reconstruction gives us a more accurate attenuation correction.

Algorithms used in iterative reconstruction involve an initial image reconstruction of the object, then some more information is added, this may be an attenuation map of the object being viewed superimposed onto the distribution of radioisotope in the object model. Then a forward calculation is done of projections after they have been updated, and, then, calculation is done of the correction factors

by comparing the original to the model (new) projections. These correction factors help in updating the model for it to be more consistent with the original data from the projection as well as the information that has been included. This process may be repeated over again, hence the name iterative.

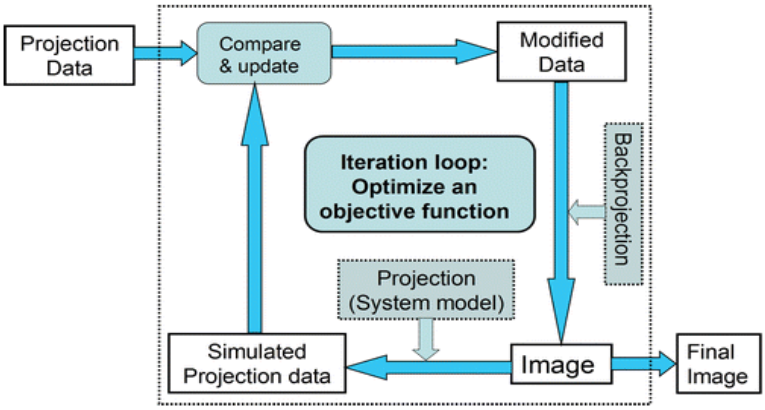

Figure 1-10 Graphical representation of the process of iterative reconstruction.

Advantages of Single-photon emission computed tomography application for radiotherapy planning.

The main advantage of the nuclear medicine medical imaging techniques (SPECT and PET) which are functional imaging modalities lies in their ability to give us information about the function of tissue in a certain body region, which often precedes the anatomical changes in the disease process.

SPECT and PET offer very good sensitivity, able to give us concentrations to the picomolar levels, for example the high specificity of ^{123}I-α-methyl-tyrosine (IMT) uptake in tumor tissue.

Another advantage is in the ability to use different tracers to target specific molecular pathways in body tissues.

Disadvantages of Single-photon emission computed tomography application for radiotherapy planning

The spatial resolution of SPECT in practice is poor compared to CT or MR. This is a big setback in radiotherapy planning because of the importance of special fidelity in radiation therapy planning.

1.4.4 Positron Emission tomography.

Like SPECT, PET uses the tracer principle which was pioneered by George Charles De Hevesy. A radiopharmaceutical is administered in the body and its distribution is detected by the nature of its radioactive decay using a gamma camera. Then following this, mathematical methods are used to construct an image. In PET the commonly used tracer is F18 fluorodeoxyglucose (FDG)

Positron emission tomography image acquisition

In PET we have an indirect method of detection. The radioactive nucleus for example ^{11}C produces a positron and becomes Boron 11. The Positron travels in tissue, losing energy along the way until it meets an electron and annihilation takes place, producing two γ rays each with energy 511 KeV moving in opposite directions. These 2 rays will travel and hit the detector at almost the same time. The time gap in which these photons are considered to be from the same event is called the coincidence window. Considering the position of the detectors involved, we get an idea of the position of the annihilation process. Other pairs of photons detected occur following the scattering of one or both photons through shallow angles, thereby remaining within an acceptable energy window but defining an erroneous line of response (scattered coincidences). A third category of paired photons is designated as randoms, due to the mistaken pairing of two independent 511 keV photons which are incident on the detectors within the specified timing window τ despite originating from two separate positron-electron annihilations. All the three are illustrated in figure 1-10.

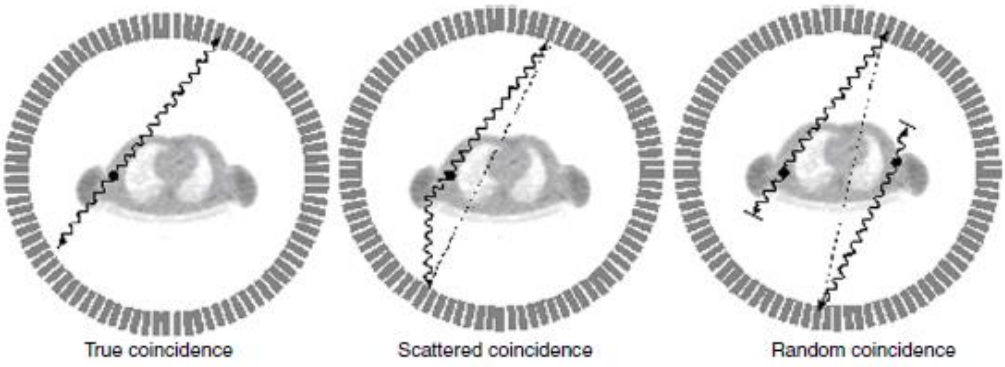

Figure 1-11 Types of coincidence events.

The narrower the timing window τ, the smaller the number of random coincidences accepted. However, as τ is made too short, true coincidences are also lost because of the nontrivial time required for photon flight, scintillation within the crystal, and electronic processing.

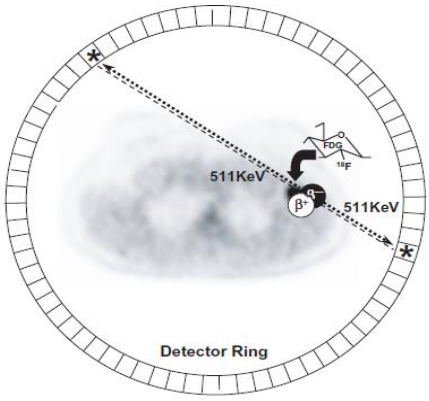

Figure 1-12 Principle of PET imaging.

In the illustration (figure 1-11), the pair of annihilation radiation photons nearly simultaneously intersect two elements within the ring of detectors (asterisks). The line that is defined by the two detectors is termed the line-of-response (dashed line).

In contrast to single-photon imaging, where collimation is required to relate a photon to its line of origin, no absorptive collimation is required in PET. This allows for far greater count-rate sensitivity than in single-photon systems. Furthermore, no degradation of resolution occurs with increasing distance from the detectors.

Just as in SPECT, the image reconstruction can be done using filtered back projection or iterative reconstruction.

SPECT and PET offer very good sensitivity, able to give us concentrations to the picomolar levels, for example the high specificity of ^{123}I-α-methyl-tyrosine (IMT) uptake in tumor tissue [28].

Another advantage is in the ability to use different tracers to target specific molecular pathways in body tissues.

The spatial resolution of SPECT and PET in practice is poor compared to CT or MR. This is a big setback in radiotherapy planning because of the importance of

special fidelity in radiation therapy planning. Because of this limitation, PET-CT and PET-MRI have been used to combine the specificity of PET and the better resolution and special fidelity of CT and MRI for radiotherapy planning.

In the International Atomic Energy Agency report 2006–2007, the experts defined the cases in which the combination of PET and CT in RT planning gives better results than using CT alone. (30) These cases include imaging in lesions that are not well defined by CT or MRI, like unsuspected lymph nodes and distant metastases, an example can be seen in figure 1-12. CT-PET is also good for minimizing the irradiation of healthy tissues, especially in lung cancer. In cases where chemotherapy is done with RT, PET-CT will help better assess the response of the cancer tissue to the treatment. This is important for "response adapted therapy" where the target volumes are adjusted during the treatment course according to the changes seen after the previous sessions.

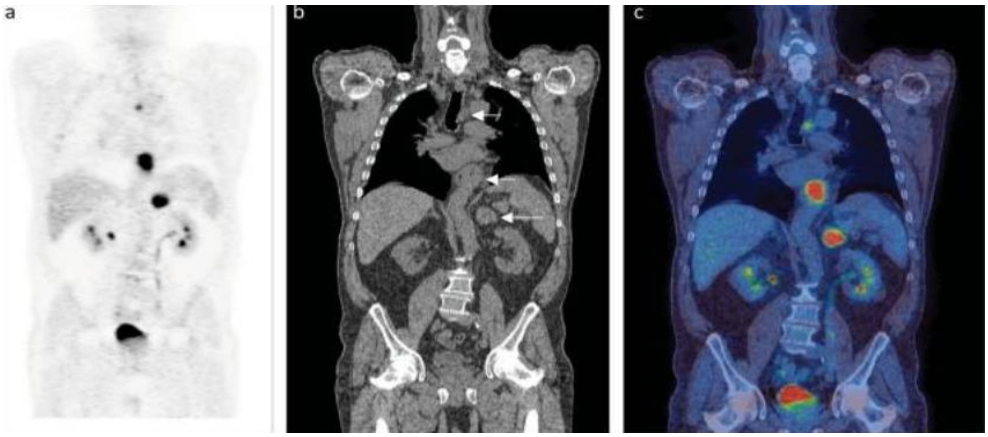

Figure 1-13 Coronal ^{18}F-FDG PET image showing increased abnormal activity in a patient with esophageal cancer with lymph node and adrenal metastases [29].

1.5 Imaging recommendations for glioma radiotherapy planning

Computed Tomography (CT) CT data from a 1 to 2mm multi-slice CT with contrast is obtained, including the region from the vertex up to foramen magnum. The different CT windows, including bones, soft tissue and orbit are used to delineate the tumor and other critical structures. CT can play a big role as an additional investigation to MRI or PET for the visualization of hemorrhagic tissue, soft tissue calcification or even bonny structures. For treatment of gliomas, target volume organ

delineation should not exclusively depend on CT imaging [31] apart from the rare cases where MRI is relatively or absolutely contraindicated, e.g. all cases of pacemakers, morphine or insulin pumps, neurostimulators, endoprostheses, granite splinters, etc. Magnetic Resonance Imaging (MRI) owing to its excellent contrast in soft tissue and the options of axial, coronal 3D, and sagittal reconstructable datasets with a small slice thickness (0.5–1.2 mm), before and after operation, MRI plays a central role in glioma target volume delineation and treatment response evaluation. MRI sequences necessary for this role include non-contrast and contrasted 3D-T1-weighted for example MP-RAGE sequences and 3D-T2-weighted sequences with thin slices e.g. fluid-attenuated inversion recovery, (FLAIR), and T2 SPACE. Low-grade gliomas are hyperintense on T2 and FLAIR sequences and hypointense on non-contrast T1 MRI sequences. Low-grade gliomas characteristically have intact blood-brain barrier, and therefore no contrast enhancement with gadolinium is seen. In low-grade gliomas with diffuse infiltration, both T2 and T1 sequences are not accurate to delineate the gross tumor volumes. They both cannot accurately differentiate between edema and tumor infiltration, or even changes following treatment from reactive gliosis. The WHO III and IV grades are characteristically contrast enhancing on T1 sequences. For example, GBM shows necrotic areas, surrounding normal tissue compression and deviation of midline. Edema around the tumor cannot be differentiated from the tumor areas with no contrast enhancement. For low- or high-grade gliomas, MRI has a high sensitivity in the diagnosis of the brain tumor but cannot specify the histology of the tumor tissue. Advances in MRI will provide significant biological information on these glioma stages and will be used in the future in bio-imaging for improvement in treatment strategies. Recent data shows that new MRI techniques can detect small changes in the organization in white matter that is using diffusion tensor imaging, and cellular proliferation and angiogenesis using diffusion MRI and MR spectroscopy [32]. Stadlbauer et al [33] used MRS to visualize the infiltration zone of gliomas. They compared the proton-MRS data with the results of stereotactic biopsies from 20 patients, and suggested that the automated

segmentation method of the lesion-related metabolic changes greatly improved tumor delineation in gliomas compared to the traditional methods.

1.5.1 Role of nuclear imaging modalities in radiotherapy planning in brain tumors.

MRI can accurately depict the anatomical map of the brain, but neither contrast enhancement of T1-weighted images nor hyperintensity seen with T2-weighted images can specifically with accuracy show the extent of the neoplastic lesions. During treatment of glioma, we see phenomena like pseudo-remission or pseudo-progression, these phenomena cannot easily be recognized using MRI, making it a weaker option for use during follow up [34]. Glioma cells which are mitotically active have increased metabolism that is, increased glycolysis, protein synthesis and DNA synthesis; [35], and these biological-molecular characteristics are what give PET a major role in accessing the actual extent of the tumor for better treatment planning [36]. In oncology, ^{18}F fluorodeoxyglucose (FDG) is generally the most widely used PET tracer but with malignant glioma, the value of FDG-PET in GTV delineation is limited, and this is due to inadequate contrast between the normal brain tissue and the tumor. Amino acid PET stands out as a better option in this role with better sensitivity and specificity, better even than MRI. The target volumes delineated in malignant glioma can significantly vary between MRI and ^{11}C-methionine (MET)-PET [35]. On the PET/MRI co-registered images, MET uptake on PET and gadolinium enhancement on T1-MRI were detected in all 39 patients (100 %). In 5 patients (13 %), MET uptake matched exactly with the gadolinium enhancement on T1-MRI. In 29 of the patients (74 %), MET uptake was located outside the gadolinium enhancement on MRI, showing additional areas of tumor infiltration. Moreover, in 27 patients (69 %), gadolinium enhancement was also located outside the MET enhancement on PET, showing that gadolinium actually correlates with post-surgery blood brain barrier disturbances and not with tumor tissue. Comparing the hyperintense areas on T2-MRI with MET uptake on PET, a difference was observed in the extent of MET uptake from the areas of

hyperintensity. In 9 of the 18 patients, MET uptake was not aligning with the hyperintensity area, and in 100 %, the region of hyperintensity T2-MRI did not align with the MET uptake areas, which was suggestive of post-surgical or tumor-related edema. Comparing the MET-PET uptake and areas of treatment failure, in 19/26 patients with a significant volume delineated by PET (above $2cm^3$) 5 of these had some part of the GTV not included in the high dose area and they all got failures in areas outside the high dose region, compared with the 14/19 patients in whom the MET-PET GTV was adequately covered and just 2 of them got treatment failure in areas outside the high dose region. It was concluded that inadequate MET-PET GTV high coverage was related with a higher risk of non-central treatment failure with a P value less than 0.01.

The half-life of ^{11}CMET being very short, requires the presence of an on-site cyclotron. ^{18} F fluoroethyl-l-tyrosine (FET) is another tracer with a longer half-life, which was found to match ^{11}C-MET in detecting biologically active tumor [40]. In a prospective single-institution trial [39] the effect of PET based radiotherapy planning on the outcome of recurrent high-grade glioma patients treated using fractionated SRT was evaluated. The average overall survival was 5 months for MRI/CT based treatment planning compared with 9 months for the amino acid PET based target volume delineation. P value = 0.03 suggesting that amino acid PET should have a significant positive impact on patient outcome.

1.6 Target organ delineation recommendations in gliomas.

T2 and FLAIR-MRI sequences are the modalities generally used for low grade Gliomas, i.e. astrocytomas, oligoastrocytomas, oligodendrogliomas Gross tumor volume (GTV) delineation [40], since these tumors characteristically don’t show contrast enhancement on T1-weighted MRIs.

It is however well known that despite the sensitivity of T2 and FLAIR MRI for tumor tissue being very high, the specificity is low. For example, the edema surrounding the tumor can be mistaken for tumor tissue, or even treatment related changes may be mistaken for active tumor tissue. At the end we may end up treating

the normal brain tissue and cause unnecessary damage and worse morbidity following treatment. Additionally, in operated patients, the GTV could include close to residual tumor non-tumoral tissue with hyperintense signal on T2 and FLAIR, e.g. post- surgery gliosis and edema. After complete tumor resection, the concept of GTV encompassing the resection cavity – as used generally in different trials and publications – is not in line with the ICRU Criteria for GTV definition: the resection cavity should be included in the clinical target volume (CTV) and not in the GTV definition. The CTV encompasses the possible microscopic tumor infiltration, including the resection cavity (in operated patients) and the surrounding normal appearing tissue in an area of 5–15 mm, excluding anatomical borders like the falx, skull, liquor areas, etc. [40]. For example, in some institutions, a distinction is made between well delineated low-grade gliomas, (the margins from GTV to CTV are ca. 5 mm), and diffuse infiltrative low-grade gliomas, (the distance from GTV to CTV larger ca. 10–15 mm).

Table 1-1. EORTC and RTOG recommendation for WHO II glioma: GTV, CTV and PTV definition [41,42].

Trial	GTV	CTV	PTV
EORTC 22033-26033/CE5	Region of high signal intensity on T2 or FLAIR MRI corresponding to the hypodense area on CT, including any areas of CT enhancement or surgical cavity + any residual tumor.	GTV + 1-1.5 cm	CTV + 5-7cm
RTOG 9802	T2 or FLAIR MRI defined tumor volume	Not defined	GTV + 1cm

The treatment fields included the T2 or FLAIR MRI-defined tumor volume plus a 2-cm margin to block edge, resulting in an approximate 1-cm dosimetric margin)

Pre- and post-surgery MRI/CT image co-registration is generally recommended. The pre-surgery GTV image significantly contributes by giving better information about the extent of the possible microscopic tumor infiltration, hence

influencing the CTV. However, in this case, the possible changes of the brain anatomy after surgery should be taken into consideration. Considering the accuracy of patient positioning done in the institution, the PTV should be defined. High-precision in low grade glioma radiation therapy is mandatory. Stereotactic radiotherapy techniques or image-guided radiotherapy have to be applied to reduce the PTV margin to 1–3 mm.

For low-grade gliomas, the total dose recommended ranges from 50.4 to 54 Gy [41] in 1.8 Gy per fraction per day, 5 days a week. From the RTOG [42] and EORTC [41] studies, it was evident that when the target volume delineation was based on the CT hypodense area, there was 52–55 % progression-free survival 5 years after radiation therapy. For the cases of local recurrence, more than 90% of the times it was located in the irradiation field.

High-Grade Gliomas (WHO III) have 2 radiological patterns described for target volume delineation [42]. The first pattern is WHO grade III gliomas with the radiological characteristics of GBM. These are best treated using T1-MRI with gadolinium contrast. The second pattern is the WHO grade III gliomas with poor contrast enhancement with gadolinium on T1-MRI. In such cases, the GTV should include the Gadolinium T1- MRI and the hyperintense areas on T2/FLAIR. The CTV margin of 1.0 to 1.5 cm should be added to the GTV. In aggressive high-grade gliomas as sometimes seen in GBM, more than 90% of the times recurrences occurred within the contrast enhancement region. In a larger portion of these patients, hyperintensity seen on T2-MRI is due to edema, and usually edema is as result of tumor compression and not macroscopic tumor invasion. Therefore, T1-MRI is more accurate for GTV delineation in such cases than T2/FLAIR.

On the other side, in group 2, WHO grade III gliomas arising from previous low-grade gliomas, we see a frequent pathological characteristic of regional malignant transformation in small islands. In this case, edema following tumor compression is very rare and when present, very small. Therefore, in these cases, it is better to include the T2/FLAIR sequences in target volume delineation because changes in T2/FLAIR are suggestive of tumor invasion. The EORTC and RTOG

clinical trials (table 1-2) were done to follow up this approach and results show that the prognosis in most of these patients is better and favorable.

Since our main goal includes sparing normal brain tissue to reduce the late side effects after radiotherapy, using multimodality imaging approach, with use of SPECT and pre-surgery MRI/CT for delineation of GTV and CTV is highly recommended. Anatomical borders must also be put in consideration. Stereotactic fixation and image-guided radiotherapy also help to reduce the PTV margin to 1–2 mm. As mentioned above, the total dose should be 59.4 Gy in 1.8 Gy per fraction 5 fractions per week. The delivery of lower doses, that is 45 to 50.4 Gy to a larger PTV delineated using T2-MRI/ FLAIR and then a higher dose to the boost region delineated using GdT1-MRI has shown good results, and tends to spare more brain tissue.

For high-Grade Gliomas (WHO IV) also called glioblastoma multiform, a CTV margin of 2 cm is usually added. Despite the local treatment approach, it should be noted that diffuse glioma usually represents a systemic brain disease at the time of diagnosis [43]. This is why the escalation of dose beyond 60Gy has a limited role as seen in many studies. However, the role of dose escalation may be seen if clear definition of a biologically relevant sub-volume or molecular disease feature calls for targeted dose escalation to a specific volume in some patients [44]. In GBM, edema surrounding the tumor in T2/FLAIR sequences, which should in many cases be suspicious of subclinical tumor cell infiltration, has been shown to lead to significantly larger irradiation volumes and doses to the whole brain when included in the GTV compared to a standard GTV to CTV margin of 2 cm without inclusion of edema, though it does not alter the central pattern of failure. Therefore, T1-MRI sequences with gadolinium contrast should be the basis for GTV delineation in GBM. Excluding the edema surrounding the tumor may significantly reduce the irradiated brain volume, but its safety in terms of efficacy and reduction in treatment-related side effects have not been demonstrated in randomized, prospective trials yet. [45] Different strategies for target volume delineation in GBM are presented in Table 2. As done in other gliomas, amino acid PET and pre-surgery MRI/CT should be co-

registered for planning and delineation of the treatment volumes. GBMs are generally treated with a total dose of 60, 2 Gy per fraction, 5 days a week [46].

Table 1-2. EORTC and RTOG glioblastoma (GBM, WHO IV): GTV, CTV and PTV definition [44].

Trial	GTV	CTV	PTV
EORTC 22981-26981/NCIC CE3, BO21990	Surgical cavity + contrast enhancing T1 abnormality.	GTV + 2-13 cm	Not defined
RTOG 0825	GTV 1 Surgical cavity + contrast enhancing T1 abnormality + T2 or FLAIR MRI abnormality GTV 2 Surgical cavity + contrast enhancing T1 abnormality.	CTV1: GTV 1+2-2.5 cm CTV 2: GTV 2 + 2cm	PTV 1: CTV 1 + 3-5 mm PTV 2: CTV 2 + 3-5mm

While delineating the organs at risk the eyes, optic chiasm, lenses, optic nerves, brainstem, inner ears, pituitary gland and hypothalamus. Not forgetting the volume of the whole brain which must be contoured to be able to evaluate the average brain dose. Some centers also recommend delineation of the hippocampi, because they help to estimate the risk of neurocognitive decline, so by using IMRT, these structures are spared as much as possible.

We therefore see the need for inclusion of SPECT or PET imaging modalities in treatment planning suggested from increased survival rates seen for patients with recurrent gliomas treated with SFRT planned with MET-PET or IMT-SPECT/CT/MRI image fusion compared with patients treated on anatomic imaging (CT and MRI) alone [47,48]. SPECT and PET are also good for the detection of early metabolic changes, which precede anatomical changes revealed by CT and MRI, and not forgetting identifying metabolically active and aggressive tumor regions, which should be treated appropriately especially with IMRT [49]. Biological imaging using 99mTc-MIBI SPECT has also been shown to modify the target volume and, hence, the treatment plan of high-grade glioma [50].

planning with the goal of delivering treatment with precision to the tumor sparing as much normal brain tissue as possible.

This study can be used to come up with recommendations for medical imaging in brain tumor treatment for application in oncology centers worldwide

4.1 Pre-research analysis.

The financial limitations in cancer treatment are a major problem especially because of the complexity of diagnosis and treatment. One of the factors that greatly contribute to this financial stress to the patients is the problem of recurrence. Recurrence is mainly a result of in accurate tumor assessment at the first treatment. If a cancer is wrongly staged due to the limitation in imaging, not only can it result in recurrence, but it can also lead to destruction of more healthy tissues at the time of treatment. These both can cause longer hospital stay and increased morbidity.

However, much use of a single modality can look inexpensive at a glance, the morbidity and mortality associated with improper diagnosis and treatment of a tumor can be even more expensive. Using a combination of imaging modalities in a multimodality imaging approach though may seem expensive will help give the doctor confidence and reduce the morbidity related to treatment failure and hence in the long run save the resources that would be wasted in remission cases.

The analog to this project is the single modality approach which is used currently, where mainly CT scan is the only imaging modality used for treatment planning. This is mainly used due to its availability but as we see in this project, the accuracy in treatment delivery is lacking which at the end is often related with more morbidity and hence more treatment costs.

This research will be useful for hospitals and oncology organizations. It will help give information that can be considered in making recommendations that can be applied in cancer institutions around the world.

4.1.1 Potential consumers of the research results

To analyze consumers of research results, it is necessary to segment the market.

Target market - the market that includes consumers interested in the results of the research who would buy the good/service connected with the student's investigation. In this research project, the target market includes the cancer hospitals, oncology departments and oncological research institutions.

4.1.2 Competitiveness analysis of technical solutions

In order to find sources of financing for the project, it is necessary, first, to determine the commercial value of the work. Analysis of competitive technical solutions in terms of resource efficiency and resource saving allows to evaluate the comparative effectiveness of scientific development. This analysis is advisable to carry out using an evaluation card.

First of all, it is necessary to analyze possible technical solutions and choose the best one based on the considered technical and economic criteria.

Evaluation map analysis presented in Table 4-1. The position of your research and competitors is evaluated for each indicator by you on a five-point scale, where 1 is the weakest position and 5 is the strongest. The weights of indicators determined by you in the amount should be 1. Analysis of competitive technical solutions is determined by the formula:

$$C = \sum P_i \cdot W_i, \tag{4.1}$$

C - the competitiveness of research or a competitor;

W_i– criterion weight;

P_i – point of i-th criteria.

The effectiveness of radiotherapy treatment for cancer patients depends greatly on the on the efficiency of the radiotherapy planning which relies on the choice of imaging modalities used in planning. Imaging is involved at various levels including, diagnoses, treatment simulation, image contouring treatment simulation, contouring and others. There are a number of imaging modalities used in radiotherapy planning and each has its own advantages and limitations for this application.

For the competitive analysis of technical solution, two imaging approaches are considered. These are:

- Single modality approach – P_i
- Multimodality approach – P_f

Single modality approach is when just a single imaging modality is used. For brain tumor radiotherapy planning, MRI is the gold standard for tumor delineation due to the good soft tissue contrast. MRI however has some limitations which include poor contrast for bonny landmarks, distorted geometry and lack of electron density data which is important for dose calculation. Computed Tomography imaging has clear visualization of high contrast bony landmarks due to the higher linear attenuation values for the bone, provides better spatial resolution and gives electron density data which is needed for dose calculation. CT imaging for radiotherapy planning offers its own set of challenges, not the least of which is it delivers extra radiation dose outside the target treatment area, and potential image artifacts. SPECT is not used as a single modality due to poor special resolution but it is very important in differentiating edema from actively growing tumor and it has a very big role in treatment response monitoring because of its ability to show tumor activity.

Because of the fact that none of the modalities gives us all the requirements for treatment planning, combination of the imaging modalities is encouraged. This will help us take advantage of the possibilities offered by the different imaging modalities as listed above.

In this research project, we are applying the multimodality imaging approach.

Table 4-1Evaluation card for comparison of competitive technical solutions

Evaluation criteria *example*	**Criterion weight**	**Points**		**Competitiveness** Taking into account weight coefficients	
1	2	3	4	7	8
Technical criteria for evaluating resource efficiency					
1. Risk of radiotherapy side effects	0,18	4	3	0,62	0,3
2. Dose homogeneity	0,13	5	4	0,56	0,5
3. Dose on organs at risk	0,2	4	3	0,8	0,39
4. Ease of planning	0,14	3	4	0,5	0,6
5. Risk of treatment failure	0,1	5	4	0,8	0,56
Economic criteria for performance evaluation					

1. Competitive methods	0,08	5	4	0,5	0,4
2. Expected lifecycle	0,07	4	4	0,35	0,35
3. Development cost	0,1	5	4	0,6	0,34
Total	**1**	**35**	**30**	**4,73**	**3,44**

The results of the competitiveness analysis show that the multimodality imaging approach is a better option in comparison with the single modality imaging approach.

4.1.3 SWOT Analysis

Complex analysis solution with the greatest competitiveness is carried out with the method of the SWOT analysis: Strengths, Weaknesses, Opportunities and Threats. The analysis has several stages.

The first stage consists of describing the strengths and weaknesses of the project, identifying opportunities and threats to the project that have emerged or may appear in its external environment. The second stage consists of identifying the compatibility of the strengths and weaknesses of the project with the external environmental conditions. This compatibility or incompatibility should help to identify what strategic changes are needed.

Table 4-2 SWOT analysis

	Strengths: S1. Increases dose to tumor sparing normal tissue. S2. Shorter treatment time with better outcome	**Weaknesses:** W1. Lack of necessary software at oncology department of hospitals.
Opportunities: O1. Treatment of patients with brain tumor. O2. Reduction in patient's treatment time	***Strategy which based on strengths and opportunities:*** 1. Reduces mortality and morbidity.	***Strategy which based on weaknesses and opportunities:*** 1. Training of medical physicists to work with the image processing and planning program.
Threats: T1. Affordability of use of a single modality compared to imaging machines that allow merging of different modalities.	***Strategy which based on strengths and threats:*** 1. Teaching the medical physicists how to manually merge images taken with different imaging machines.	***Strategy which based on weaknesses and threats:*** 1. Use of the available software systems to merge images.

From this analysis in the matrix, it can be concluded that this project is viable since the strengths and opportunities in the project are greater than the weaknesses

and threats.

4.2 Project Initiation

In the initiation processes, the initial purpose and content of the project are determined. The initial financial resources are fixed. The internal and external stakeholders of the project are determined, which will interact and influence the overall result of the research project are determined.

4.2.1 Project Goals and Results

Project stakeholders are persons or organizations that are actively involved in the project or whose interests may be affected both positively and negatively during the execution or as a result of the completion of the project. They can be contractors, sponsors, the public, etc. Information about the stakeholders of the project is presented in the table below.

Table 4-3 Stakeholders of the project

Stakeholders of the project	**Stakeholders of the project expectations**
Cancer hospitals/clinics	Reduced patient mortality and morbidity; Reduced expenditure on treatment;
Research Institutions	Better treatment outcome; Reduce overall expenditure on treatment;
Tomsk Polytechnic University (TPU)	The acquired results will make way for better treatment approach. And open more research opportunities in TPU.

Information about the hierarchy of project goals and criteria for achieving goals is given in the table below.

Table 4-4 Project goals and results

Project goals	To study the possibilities of multimodality imaging application for brain tumors radiotherapy planning.
Expected results of the project	Based on the conducted research, the treatment volumes delineated using the different imaging modalities are compared. The results are analyzed and recommendations are given.
Acceptance criteria of the project result	Efficiency in relation to the proposed measures to improve the quality of radiotherapy treatment and ensure maximum dose to the target tumor.
Requirements to the project	The project is completed on time.
	Stability of technological equipment.

results	The efficiency of the equipment used.
	The results are used to improve treatment planning for cancer patients. That is, to reduce doses to critical organs while ensuring maximum dose to the target volume.

4.2.2 Organizational Structure of the Project

The organizational structure of the project involves all participants or people who participated in the research work, the number of hours they spent and the roles they played in the research. In this research work, there were two participants. The organizational structure of the project is presented in the table below.

Table 4-5 Project Working Group

№	**Name**	**Role in the Project**	**Functions**	**Hours spent** (working days (from table 4-7) × 6 hours)
1	Ph.D. Irina Miloichikova	Project Manager	Coordination of work activities, guidance and assistance in project implementation. Verification of results obtained.	100
2	Ategyeka Mutambi	Project Executor	Work on project implementation.	750
Total:				850

4.3 Assumptions and constraints

Limitations and assumptions are summarized in table below.

Table 4-6 Limitations and assumptions

Factor	**Limitations/assumptions**
1. Project budget - for design	550000 Rubles
1.1 Source of budgeting	State financing TPU
2. Project timeline:	1 February 2022 – 20 May 2022
2.1 Date of approval of the project management plan	12 February 2022
2.2 Project completion date	20 May 2022

As a result of the initialization of the project, the goals and expected results were formulated, the stakeholders of the project and the financial framework were identified, which is very important for the successful completion of the project and its implementation.

4.3.1 Planning of Scientific and Technical Project Management

The planning process group consists of the processes that are carried out to determine the overall content of the work, clarify the goals, and develop the sequence of actions required to achieve these goals.

The scientific project management plan should include the following elements.

4.3.2 Hierarchical structure of project activities

Hierarchical Work Structure (HWS) - detailing the enlarged work structure. In the process of creating an HWS, the content of the entire project is structured and defined. It may be presented in schemes.

4.3.3 Deadlines for the project stages

Project Schedule

As part of planning a science project, you need to build a project timeline and a Gantt Chart.

Table 4-7 Project duration and timeline for various processes.

Job title	Duration, working days	Start date	Date of completion	Participants
Drawing up the technical assignment	5	1/02/2022	5/02/2022	Project Manager
Literature review	15	6/02/2022	20/02/2022	Project Executor
Calendar planning	2	21/02/2022	22/02/2022	Project manager Project Executor
Research method/procedure	3	23/02/2022	25/02/2022	Project manager
Image processing	9	14/03/2022	24/03/2022	Project Executor
Contouring	26	25/03/2022	29/04/2022	Project manager Project Executor
Analysis of the results	7	30/04/2022	06/05/2022	Project manager Project Executor
Summary of	3	09/05/2022	11/05/2022	Project

results				Executor
Evaluation of the effectiveness of the results	3	11/05/2022	13/05/2022	Project manager Project Executor
Drawing up a final report	10	14/05/2022	23/05/2022	Project Executor
Defense Preparation	8	24/05/2022	31/05/2022	Project Executor

A Gantt chart, or harmonogram, is a type of bar chart that illustrates a project schedule. This chart lists the tasks to be performed on the vertical axis, and time intervals on the horizontal axis. The width of the horizontal bars in the graph shows the duration of each activity.

Table 4-8 Gantt chart showing the timeline of the project

	Activities	Participants	T_c, days	Duration of the project											
				February			March			April			May		
	Drawing up the technical assignment	Project manager													
	Literature review	Project Executor	**5**												
	Calendar planning	Project manager, Project Executor													
	Research method/procedure	Project manager													
	Contouring	Project Executor													
	Planning	Project manager, Project Executor	**6**												

	Analysis of the results	Project manager, Project Executor													
	Summary of results	Project Executor													
	Evaluation of the effectiveness of the results	Project manager Project Executor													
0	Drawing up a final report	Project Executor	**0**												
	Defense Preparation	Project Executor													

- Project manager

- Project Executor

Thus, the duration of the task performed by the student and the supervisor. In general, the duration of work in calendar days for a student is 83 days, and for a supervisor is 46 days. The total number of working days is 91.

4.3.4 Scientific and Technical Research Budget

The project budget fully reflects all types of planned expenditures necessary fir the implementation of the project. To find the final cost value, all calculated costs for individual items related to the manager and the executer are summed. These costs include office supplies, printing costs, various equipment required for paperwork, and all costs that are associated with the purchase of special equipment (for example, instruments, instrumentation, stands, devices and mechanisms) necessary for the project.

The calculation of material costs may be also carried out according to the formula:

$$C_m = (1 + k_T) \cdot \sum_{i=1}^{m} P_i \cdot N_{consi}, \quad (4.2)$$

where

m – the number of types of material resources consumed in the performance of scientific research;

N_{consi} – the amount of material resources of the i-th species planned to be used when performing scientific research (units, kg, m, m^2, etc.);

P_i – the acquisition price of a unit of the i-th type of material resources consumed (rub./units, rub./kg, rub./m, rub./m^2, etc.);

k_T – coefficient taking into account transportation costs.

Prices for material resources can be set according to data posted on relevant websites on the Internet by manufacturers (or supplier organizations).

Table 4–9 shows the costs of all items.

Table 4-9 Costs of specialized equipment and other materials

Name	Unit per measurement	Quantity (units, amount)	Price per unit (rubles)	Sum (rubles)
Stationaries	Unit	1 each	1,000	1,000
Transportation	Unit	70	50	3,500
Printing	Page	200	5	1,000
Folder	Unit	2	10	20
Stapler	Unit	1	200	200
Staples	Pack	1	50	50
Hole puncher	Unit	1	300	300
Laptop	Unit	1	40000	40000
Microsoft windows 10 professional RU x 64	Unit	1	5000	5000
Kaspersky anti-virus	Unit	1	2000	2000
			Total costs for materials Total transportation and purchasing costs (3-5%) Total costs per article, C_m	53070

4.3.5 Calculation of the Depreciation

The cost of specialized equipment is recorded in the form of depreciation charges. Depreciation is a reduction in the value of an asset over time, due in particular to wear or tear. To calculate the total depreciation of the specialized equipment, the annual depreciation is calculated first, then the monthly depreciation, according the number of working days the equipment was used. The annual depreciation is

calculated using the following formula:

$N_D = \frac{1}{T} \cdot 100\%$, where T is the expected lifetime in years.

The life time of the laptop is approximately 10 years, the Microsoft Windows 10 license is 4 years and the anti-virus software is 1 year.

Then the annual depreciation rate for each of them respectively, is:

$$N_D = \frac{1}{10} \cdot 100\% = 10\ \%,$$

$$N_D = \frac{1}{4} \cdot 100\% = 25\ \%,$$

$$N_D = \frac{1}{1} \cdot 100\% = 100\ \%$$

The daily depreciation is estimated based on the number of days the equipment is used. In this project, it is assumed that each specialized equipment is used for a period of 5 months, which is 150 days. Hence, the depreciation is calculated as such:

$D_L = P \cdot \frac{N_D}{100} \cdot \frac{T}{365}$, where P is the cost of the equipment, is the annual depreciation and T is the period of use in months.

$$D_L = 40000 \cdot \frac{N_D}{100} \cdot \frac{T}{365} = 40000 \cdot \frac{10}{100} \cdot \frac{150}{365} = 1643{,}84 \text{ RUB},$$

$$D_{Win10} = 5000 \cdot \frac{N_D}{100} \cdot \frac{T}{365} = 5000 \cdot \frac{25}{100} \cdot \frac{150}{365} = 513{,}7\ RUB,$$

$$D_{SS} = 2000 \cdot \frac{N_D}{100} \cdot \frac{T}{365} = 2000 \cdot \frac{100}{100} \cdot \frac{150}{365} = 821{,}92 \text{ RUB},$$

The sum of depreciation for all equipment is:

D = 2979,46

4.3.6 Basic Salary

The basic salary includes the basic salary of scientific and engineering workers, and all other participants directly involved in the performance of this project. The amount of salary expenses is determined based on the labor intensity of the work performed and the current system of remuneration. The basic salary includes a bonus

paid monthly from the salary fund (the amount is determined by the Regulations on Remuneration of Labor).

The basic salary (S_b) is calculated according to the following formula:

$$S_b = S_a \cdot T_w , \qquad 4(4.3)$$

where S_b – basic salary per participant;

T_w – the duration of the work performed by the scientific and technical worker, working days;

S_a - the average daily salary of a participant, rub.

The average daily salary for a 5-day working week is calculated by the formula:

$$S_d = \frac{S_m \cdot M}{F_v} , \qquad (4.4)$$

where S_m – monthly salary of a participant, rub.;

M – the number of months of work without leave during the year:

at holiday in 48 days, M = 11.2 months, 6 day per week;

- – valid annual fund of working time of scientific and technical personnel (251 days).

Table 4-10 The valid annual fund of working time

Working time indicators	
Calendar number of days	365
The number of non-working days - weekend - holidays	 52 14
Loss of working time - vacation - isolation period - sick absence	 48
The valid annual fund of working time	251

Monthly salary is calculated by formula:

$$S_{month} = S_{base} \cdot (k_{premium} + k_{bonus}) \cdot k_{reg} , \qquad (4.5)$$

where S_{base} – base salary, rubles;

$k_{premium}$ – premium rate;

k_{bonus} – bonus rate;

k_{reg} – regional rate.

Assuming, an associate professor of technical sciences, working at TPU has a salary equal to 40000 rubles and a medical physicist with no experience in Tomsk has an average salary of 20000 rubles. With this in mind, the total salary of the project manager and project executor is calculated

Monthly salaries:

- For project supervisor:

$$S_{month} = S_{base} \cdot (k_{\text{premium}} + k_{bonus}) \cdot k_{reg} = 40000 \cdot (1{,}3 + 0{,}25) \cdot 1{,}3 = 80600 \text{ RUB}$$

- For project executor:

$$S_{month} = S_{base} \cdot \left(k_{\text{premium}} + k_{bonus}\right) \cdot k_{reg} = 20000 \cdot (1{,}3 + 0{,}25) \cdot 1{,}3 = 40300 \text{ RUB}$$

Table 4-11 Calculation of the base salaries

Performers	S_{base}, rubles	$k_{premium}$	k_{bonus}	k_{reg}	S_{month}, rub.	W_d, rub.	T_p, work days	W_{base}, rub.
Project manager	40000	1,3	0,25	1,3	80600	2686,67	46	123586,82
Project executor	20000				40300	1343,33	83	111496,67
Total								235083,49

4.3.7 Additional Salary

This point includes the amount of payments stipulated by the legislation on labor, for example, payment of regular and additional holidays; payment of time associated with state and public duties; payment for work experience, etc.

Additional salaries are calculated on the basis of 10-15% of the base salary of workers:

$$W_{add} = k_{extra} \cdot W_{base} \quad (4.6)$$

where W_{add} – additional salary, rubles;

k_{extra} – additional salary coefficient (10%);

W_{base} – base salary, rubles.

Table 4-12 Additional Salary

Participant	Additional Salary, rubles
Project manager	12358,68
Project executor	11149,67
Total	23508,35

4.3.8 Social Security Pays (Labor Tax)

Social security pays/labor tax, to extra-budgetary funds are compulsory according to the norms established by the legislation of the Russian Federation to the state social insurance (SIF), pension fund (PF) and medical insurance (FCMIF) from the costs of workers. Payment to extra-budgetary funds is determined by the formula:

$$P_{social} = k_b \cdot (W_{base} + W_{add}) \tag{4.7}$$

where k_b – coefficient of deductions for labor tax.

In accordance with the Federal law of July 24, 2009 No. 212-FL, the amount of insurance contributions is set at 30,2%. Institutions conducting educational and scientific activities have rate – 27,1%.

Table 4-13 Labor tax

	Project manager	Project executor
Coefficient of deductions	30,2%	
Salary (basic and additional), rubles	135945,5	122646,34
Labor tax, rubles	40783,65	36793,9
Total		77577,55

4.3.9 Overhead Costs

Overhead costs include other management and maintenance costs that can be allocated directly to the project. In addition, this includes expenses for the maintenance, operation and repair of equipment, production tools and equipment, buildings, structures, etc.

Overhead costs account from 30% to 90% of the amount of base and additional salary of employees.

Overhead is calculated according to the formula:

$$C_{ov} = k_{ov} \cdot (W_{base} + W_{add})$$

where k_{ov} – overhead rate.

Table 4-14 Overhead cost

	Project leader	Engineer
Overhead rate	50%	
Salary, rubles	135945,5	122 646,34
Overhead, rubles	67972,75	61 323.17
Total		129 295,92

4.3.10 Other Direct Costs

Energy costs for equipment are calculated by the formula:

$$C = P_{el} \cdot P \cdot F_{eq}$$

where

– power rates (5.8 rubles per 1 kWh);

– power of equipment, kW;

– equipment usage time, hours.

Table 4-15 Other direct costs

	Power rates, kWh	Power of equipment, kW	Equipment usage time, hr	Energy cost, rubles
Computer for TPS	5.8	0.5	123	356,70
Laptop	5.8	0.5	492	1426,80
Total				1783,50

Formation of Budget Costs

The calculated cost of research is the basis for budgeting project costs.

Determining the budget for the scientific research is given in the table 1.14 below.

Table 4-16 Items expenses grouping

Name	Cost, rubles
• Material costs	6070,00
• Equipment costs	53070,00
• Basic salary	235083,49
• Additional salary	23508,35
• Labor tax	70078,39
• Overhead	129295,92
• Other direct costs	1783,50
Total planned costs	**518890**

4.4 Determination of Resource (resource-saving), financial, budgetary, social and economic efficiency of research

The effectiveness of a scientific resource-saving project includes social efficiency, economic and budgetary efficiency. Public efficiency indicators take into account the socio-economic consequences of the implementation of an investment project for society as a whole, including the direct results and costs of the project, as well as costs and benefits in related sectors of the economy, environmental, social and other non-economic effects. The indicators of the economic efficiency of the project take into account the financial implications of its implementation for the enterprise implementing the project. In this case, the performance indicators of the project as a whole characterize from an economic point of view, technical, technological and organizational design solutions. Budgetary efficiency is characterized by the participation of the state in the project in terms of expenditures and revenues of budgets of all levels. In addition to the above types of efficiency, the resource effect can be distinguished (characterized by indicators reflecting the influence of innovation on the volume of production and consumption of one or another type of resource), scientific and technical (evaluated by indicators of novelty and usefulness), etc.

4.4.1 Evaluation of the Absolute Effectiveness of the Project

Determination of efficiency is based on the calculation of the integral indicator of the effectiveness of scientific research. Its finding is associated with the definition of two weighted average values: financial efficiency and resource efficiency.

The integral indicator of the financial efficiency of a scientific study is obtained in the course of estimating the budget for the costs of three (or more) variants of the execution of a scientific study. For this, the largest integral indicator of the implementation of the technical problem is taken as the calculation base (as the denominator), with which the financial values for all the options are correlated.

The integral financial measure of development is defined as:

$$I_f^p = \frac{F_{p_i}}{F_{max}}$$

where I_f^p – integral financial indicator of current project;

F_{p_i} – price of i-th variant of execution;

F_{max} – the maximum cost of execution of the research project (including analogues).

In this project, $F_{p_i} = 518890$. It is assumed that, $F_{max} = 550000$.

Hence, the integral financial indicator is:

$$I_f^p = \frac{518890}{550000} = 0{,}94$$

The resulting value of the integral financial indicator of development reflects the corresponding numerical increase in the budget of development costs in times (a value greater than one), or the corresponding numerical reduction in the cost of development in times (a value less than one, but higher than zero). The integral financial indicator is equal to 0,94. This means that, the corresponding numerical reduction in the cost of development times is 0,94.

The integral indicator of the resource efficiency of the variants of the research object can be determined as follows:

$$I_m^a = \sum_{i=1}^{n} a_i b_i^a \qquad I_m^p = \sum_{i=1}^{n} a_i b_i^p$$

where I_m – integral indicator of resource efficiency for the i-th version of the development;

a_i– the weighting factor of the i-th version of the development;

b_i^a, b_i^p– score rating of the i-th version of the development, is established by an expert on the selected rating scale;

n – number of comparison parameters.

The calculation of the integral indicator of resource efficiency is presented in the form of table 4-17.

Table 4-17 Evaluation of the performance of the project

Criteria	Weight criterion	Points	
		I_m^p	I_m^a
1. Risk of radiotherapy side effects	0,18	5	3
2. Accurate delineation of tumour volume	0,13	4	4
3. Delineation of organs at risk	0,2	5	5
4. Ease of contouring	0,14	4	4
5. Risk of treatment failure	0,1	5	4
Economic criteria for performance evaluation			
1. Competitive methods	0,08	4	4
2. Expected lifecycle	0,07	5	5
3. Development cost	0,1	4	4
Total	**1**	**4,55**	**4,09**

$$I^p{}_m = \sum_{i=1}^{n} a_i b_i^a$$

$$I^p{}_m = (0{,}18 \times 5) + (0{,}13 \times 4) + (0{,}2 \times 5) + (0{,}14 \times 4) + (0{,}1 \times 5) + (0{,}08 \times 4) + (0{,}07 \times 5) + (0{,}1 \times 4)$$

$$I^p{}_m = 4{,}55$$

$$I^a{}_m = \sum_{i=1}^{n} a_i b_i^a$$

$$I^a{}_m = (0{,}18 \times 3) + (0{,}13 \times 4) + (0{,}2 \times 5) + (0{,}14 \times 4) + (0{,}1 \times 4) + (0{,}08 \times 4) + (0{,}07 \times 5) + (0{,}1 \times 4)$$

$$I^a{}_m = 4{,}09$$

The integral efficiency indicator of the scientific research project (I_{fin}^p) and of the analog (I_{fin}^a) is determined according to the formula of the integral basis of the financial integral resource efficiency:

$$I_{fin}^a = \frac{I_m^a}{I_f^a};\ I_{fin}^p = \frac{I_m^p}{I_f^p};$$

$$I_{fin}^a = \frac{4{,}09}{1} = 4{,}09;\ I_{fin}^p = \frac{4{,}55}{0{,}93} = 4{,}89$$

Comparison of the integral indicator of the efficiency of the current project and analogs will determine the comparative efficiency the project. Comparative project efficiency:

$$E_{av} = \frac{I_{fin}^{p}}{I_{fin}^{a}}$$

Where E_{av} - is the comparative project efficiency; I_{fin}^{p} - integral indicator of project; I_{fin}^{a} - integral indicator of the analog.

$$E_{av} = \frac{4{,}89}{4{,}09} = 1{,}20$$

Thus, the effectiveness of the development is presented in table 4-18.

Table 4-18 Comparative efficiency of the project.

Indicators	**Points**	
	Project	Analog
Integral resource efficiency indicator	4,55	4,09
Integral performance indicator for the variants	4,89	4,09
Comparative performance of the variants	1	1

Comparison of the values of integral performance indicators allows project managers and executors to understand and choose a more effective solution to the technical problem based on the financial and resource efficiency.

Conclusion

In this section, stages for design and create competitive development that meet the requirements in the field of resource efficiency and resource saving were developed.

These stages include:

- development of a common economic project idea, formation of a project concept;
- organization of work on a research project;
- identification of possible research alternatives;
- research planning;
- assessing the commercial potential and prospects of scientific research from the standpoint of resource efficiency and resource saving;
- determination of resource (resource saving), financial, budget, social and economic efficiency of the project.

References

1. Stupp, R., Mason, W. P., Van Den Bent, M. J., Weller, M., Fisher, B., Taphoorn, M. J., ... & Mirimanoff, R. O. (2005). Radiotherapy plus concomitant and adjuvant temozolomide for glioblastoma. New England journal of medicine, 352(10), 987-996.
2. Wick, W., Hartmann, C., Engel, C., Stoffels, M., Felsberg, J., Stockhammer, F., ... & Weller, M. (2009). NOA-04 randomized phase III trial of sequential radiochemotherapy of anaplastic glioma with procarbazine, lomustine, and vincristine or temozolomide. Journal of clinical oncology, 27(35), 5874.
3. Cairncross, G., Wang, M., Shaw, E., Jenkins, R., Brachman, D., Buckner, J., ... & Mehta, M. (2013). Phase III trial of chemoradiotherapy for anaplastic oligodenPh.Doglioma: long-term results of RTOG 9402. Journal of clinical oncology, 31(3), 337.
4. Ferlay, J., Shin, H. R., Bray, F., Forman, D., Mathers, C., & Parkin, D. M. (2010). Estimates of worldwide burden of cancer in 2008: GLOBOCAN 2008. International journal of cancer, 127(12), 2893-2917.
5. Louis, D. N., Ohgaki, H., Wiestler, O. D., Cavenee, W. K., Burger, P. C., Jouvet, A., ... & Kleihues, P. (2007). The 2007 WHO classification of tumours of the central nervous system. Acta neuropathologica, 114(2), 97-109.
6. Grech, N., Dalli, T., Mizzi, S., Meilak, L., Calleja, N., & Zrinzo, A. (2020). Rising incidence of glioblastoma multiforme in a well-defined population. Cureus, 12(5).
7. Louis, D. N., Ohgaki, H., Wiestler, O. D., Cavenee, W. K., Burger, P. C., Jouvet, A., ... & Kleihues, P. (2007). The 2007 WHO classification of tumours of the central nervous system. Acta neuropathologica, 114(2), 97-109.
8. Komori, T. (2022). The 2021 WHO classification of tumors, central nervous system tumors: the 10 basic principles. Brain Tumor Pathology, 1-4.
9. Miller, Kimberly D., et al. "Brain and other central nervous system tumor statistics, 2021." CA: a cancer journal for clinicians 71.5 (2021): 381-406.)

10. Khan, Faiz M., et al. Khans treatment planning in radiotherapy. 4 e. 4. Hong Kong: Wolters Kluwer, 2016. pp. 39-44.
11. Subburaj K, Ravi B, Agarwal M. Automated identification of anatomical landmarks on 3D bone models reconstructed from CT scan images. s.l. : compmedimag, 2019. 19345065..
12. Jiang Hsieh, Eugene Liu, Brian Nett, Jie Tang, Jean-Baptiste Thibault, Sonia Sahney**.** A new era of imagereconstruction: TrueFidelity. s.l. : Imagination at wor, 2019.
13. Barrett, Julia F.Keat, Nicholas. Artifacts in CT: Recognition and Avoidance. 6, s.l. : RadioGraphics, 2014, Vol. 24. 0271-5333.
14. Kim C, Pua R, Lee CH, et al. An additional tilted-scan-based CT metal-artifact-reduction method for radiation therapy planning. 20(1):237-249. doi:10.1002/acm2, s.l. : J Appl Clin Med Phys, 2019. 12523.
15. Curtis B Caldwell, Katherine Mah, Matthew Skinner, Cyril E Danjoux. Can PET provide the 3D extent of tumor motion for individualized internal target volumes? A phantom study of the limitations of CT and the promise of PET,. 5, s.l. : International Journal of Radiation Oncology Biology Physics, 2003, Vol. 55. Pages 1381-1393, ISSN 0360-3016.
16. Park, Sang-June, et al. “Evaluation of the combined effects of target size, respiratory motion and background activity on 3D and 4D {PET}/{CT} images. 13, s.l. : Physics in Medicine and Biology, 2008, Vol. 53. 3661-3679.
17. Hardy, By Kathy. MRI-Guided Radiation Therapy.Spring City : Radiology today, radiologytoday.net, Great Valley Publishing Company, September 2014, Vol. Vol. 15 No. 9 P. 20.
18. Tuncbilek, Nermin, Karakas, Hakki Muammer,Okten, Ozerk Omur. Dynamic contrast enhanced MRI in the differential diagnosis of soft tissue tumors. 3, s.l. : European Journal of Radiology, 2005, Vol. 53. 0720-048X.
19. Leung D, Han X, Mikkelsen T, Nabors LB. Role of MRI in primary brain tumor evaluation. s.l. : J Natl Compr Canc Netw, 2014 Nov, Vols. 1561-8. doi: 10.6004/jnccn.2014.0156. 25361803.

20. Manaster, B. J. Soft-Tissue Masses: Optimal Imaging Protocol and Reporting. 3, s.l. : American Journal of Roentgenology, 2013/09/01, Vol. 201. 0361-803X.
21. Broadhouse, Kathryn Mary. "The physics of MRI and how we use it to reveal the mysteries of the mind." Front. Young Minds 7 (2019): 23.
22. Owrangi AM, Greer PB, Glide-Hurst CK. MRI-only treatment planning: benefits and challenges. Phys Med Biol. 2018 Feb;63(5) 05TR01. doi:10.1088/1361-6560/aaaca4. PMID: 29393071; PMCID: PMC5886006.
23. Chin S, Eccles CL, McWilliam A, Chuter R, Walker E, Whitehurst P, Berresford J, Van Herk M, Hoskin PJ, Choudhury A. Magnetic resonance-guided radiation therapy. 1, s.l. : J Med Imaging Radiat Oncol, 2020 Feb, Vol. 64, pp. 163-177. Epub 2019 Oct 23. PMID: 31646742..
24. Kurz, Christopher,Buizza, Giulia,LanPh.Dy, Guillaume,Kamp, Florian,Rabe, Moritz. Medical physics challenges in clinical MR-guided radiotherapy.s.l. : Radiation onchology, 2020, Vol. 15. https://doi.org/10.1186/s13014-020-01524-4.
25. Amy, Walker, and Liney Gary**.** MRI distortion: considerations for MRI based radiotherapy treatment planning. 103-113. doi.org, s.l. : Australasian Physical & Engineering Sciences in Medicine, 2014, Vol. 37.
26. van der Heide, Uulke A,Frantzen-Steneker.MRI basics for radiation oncologists. s.l. : Clinical and Translational Radiation Oncology, 2019, Vol. 18. 2405-6308. Livieratos, L. (2012).
27. Glaudemans, Andor WJM, and Alberto Signore. "Nuclear medicine imaging modalities: bone scintigraphy, PET-CT, SPECT-CT." Bone Metastases. Springer, DorPh.Decht, 2014. 71-94.
28. Grosu, A. L., Feldmann, H. J., Dick, S., Dzewas, B., Nieder, C., Gumprecht, H., ... & Weber, W. A. (2002). Implications of IMT-SPECT for postoperative radiotherapy planning in patients with gliomas. International Journal of Radiation Oncology* Biology* Physics, 54(3), 842-854.
29. Cook, G. J. (2012). PET/CT in oncology. Clinical medicine, 12(4), 368.

30. MacManus, M., Nestle, U., Rosenzweig, K. E., Carrio, I., Messa, C., Belohlavek, O., ... & Jeremic, B. (2009). Use of PET and PET/CT for radiation therapy planning: IAEA expert report 2006–2007. Radiotherapy and oncology, 91(1), 85-94.
31. Fiorentino, A., Caivano, R., Pedicini, P., & Fusco, V. (2013). Clinical target volume definition for glioblastoma radiotherapy planning: magnetic resonance imaging and computed tomography. Clinical and Translational Oncology, 15(9), 754-758.
32. Price, S. J., & Gillard, J. H. (2011). Imaging biomarkers of brain tumour margin and tumour invasion. The British journal of radiology, 84(special_issue_2), S159-S167.
33. Brandsma, D., Stalpers, L., Taal, W., Sminia, P., & van den Bent, M. J. (2008). Clinical features, mechanisms, and management of pseudoprogression in malignant gliomas. The lancet oncology, 9(5), 453-461.
34. Stadlbauer, A., Buchfelder, M., Doelken, M. T., Hammen, T., & Ganslandt, O. (2011). Magnetic resonance spectroscopic imaging for visualization of the infiltration zone of glioma. Central European Neurosurgery-Zentralblatt für Neurochirurgie, 72(02), 63-69.
35. Demetriades, A. K., Almeida, A. C., Bhangoo, R. S., & Barrington, S. F. (2014). Applications of positron emission tomography in neuro-oncology: a clinical approach. the surgeon, 12(3), 148-157.
36. Götz, L., Spehl, T. S., Weber, W. A., & Grosu, A. L. (2012). PET and SPECT for radiation treatment planning. The Quarterly Journal of Nuclear Medicine and Molecular Imaging: Official Publication of the Italian Association of Nuclear Medicine (AIMN)[and] the International Association of Radiopharmacology (IAR), [and] Section of the Society of., 56(2), 163-172.
37. Grosu, A. L., Weber, W. A., Riedel, E., Jeremic, B., Nieder, C., Franz, M., ... & Molls, M. (2005). L-(methyl-11C) methionine positron emission tomography for target delineation in resected high-grade gliomas before radiotherapy. International Journal of Radiation Oncology* Biology* Physics, 63(1), 64-74.

38. Lee, I. H., Piert, M., Gomez-Hassan, D., Junck, L., Rogers, L., Hayman, J., ... & Tsien, C. (2009). Association of 11C-methionine PET uptake with site of failure after concurrent temozolomide and radiation for primary glioblastoma multiforme. International Journal of Radiation Oncology* Biology* Physics, 73(2), 479-485.
39. Grosu, A. L., Weber, W. A., Franz, M., Stärk, S., Piert, M., Thamm, R., ... & Nieder, C. (2005). Reirradiation of recurrent high-grade gliomas using amino acid PET (SPECT)/CT/MRI image fusion to determine gross tumor volume for stereotactic fractionated radiotherapy. International Journal of Radiation Oncology* Biology* Physics, 63(2), 511-519.
40. Grosu, A. L., Astner, S. T., Riedel, E., Nieder, C., Wiedenmann, N., Heinemann, F., ... & Weber, W. A. (2011). An interindividual comparison of O-(2-[18F] Fluoroethyl)-L-Tyrosine (FET)–and L-[Methyl-11C] methionine (MET)–PET in patients with brain gliomas and metastases. International Journal of Radiation Oncology* Biology* Physics, 81(4), 1049-1058.
41. Fairchild, A., Weber, D. C., Bar-Deroma, R., Gulyban, A., Fenton, P. A., Stupp, R., & Baumert, B. G. (2012). Quality assurance in the EORTC 22033–26033/CE5 phase III randomized trial for low grade glioma: the digital individual case review. Radiotherapy and Oncology, 103(3), 287-292.
42. Shaw, E., Arusell, R., Scheithauer, B., O'fallon, J., O'neill, B., Dinapoli, R., ... & Abrams, R. (2002). Prospective randomized trial of low-versus high-dose radiation therapy in adults with supratentorial low-grade glioma: initial report of a North Central Cancer Treatment Group/Radiation Therapy Oncology Group/Eastern Cooperative Oncology Group study. Journal of Clinical Oncology, 20(9), 2267-2276.
43. van den Bent, M. J., Brandes, A. A., Taphoorn, M. J., Kros, J. M., Kouwenhoven, M. C., Delattre, J. Y., ... & Hoang-Xuan, K. (2013). Adjuvant procarbazine, lomustine, and vincristine chemotherapy in newly diagnosed anaplastic oligodenPh.Doglioma: long-term follow-up of EORTC brain tumor group study 26951. Journal of clinical oncology, 31(3), 344-350.

44. Whitfield, G. A., Kennedy, S. R., Djoukhadar, I. K., & Jackson, A. (2014). Imaging and target volume delineation in glioma. Clinical Oncology, 26(7), 364-376.
45. Sahm, F., Capper, D., Jeibmann, A., Habel, A., Paulus, W., Troost, D., & Von Deimling, A. (2012). AdPh.Dessing diffuse glioma as a systemic brain disease with single-cell analysis. Archives of neurology, 69(4), 523-526.
46. Nieder, C., & Mehta, M. P. (2011). Advances in translational research provide a rationale for clinical re-evaluation of high-dose radiotherapy for glioblastoma. Medical hypotheses, 76(3), 410-413.
47. Grosu, Anca L., et al. "Reirradiation of recurrent high-grade gliomas using amino acid PET (SPECT)/CT/MRI image fusion to determine gross tumor volume for stereotactic fractionated radiotherapy." International Journal of Radiation Oncology* Biology* Physics 63.2 (2005): 511-519
48. Kracht, L. W., Miletic, H., Busch, S., Jacobs, A. H., Voges, J., Hoevels, M., ... & Heiss, W. D. (2004). Delineation of brain tumor extent with [11C] L-methionine positron emission tomography: local comparison with stereotactic histopathology. Clinical Cancer Research, 10(21), 7163-7170
49. Valotassiou, V., Leondi, A., Angelidis, G., Psimadas, D., & Georgoulias, P. (2012). SPECT and PET imaging of meningiomas. The Scientific World Journal, 2012
50. Krengli, M., Loi, G., Sacchetti, G., Manfredda, I., Gambaro, G., Brambilla, M., ... & Inglese, E. (2007). Delineation of target volume for radiotherapy of high-grade gliomas by 99m Tc-MIBI SPECT and MRI fusion. Strahlentherapie und Onkologie, 183(12), 689-694
51. Chernov, Vladimir I., et al. "The first experience of using 99m TC-1-THIO-d-glucose for single-photon emission computed tomography imaging of lymphomas." Сибирский онкологический журнал 17.4 (2018): 81-87.
52. Rasch C, Keus R, Pameijer F, et al. The potential impact of CT±MRI matching on tumor volume delineation in advanced head and neck cancer. Int J Radiat Oncol Biol Phys 1997; 39:841±848.

53. Federal Law "On the Fundamentals of Labor Protection in the Russian Federation" of 17.07.99 № 181 – FZ.
54. SanPiN 2.2.2 / 2.4.1340-03. Sanitary-epidemiological rules and standards "Hygienic requirements for personal electronic computers and work organization".
55. GOST 12.1.038-82 Occupational safety standards system. Electrical safety.
56. Fire and explosion safety of industrial facilities. GOST R12.1.004-85 Occupational safety standards system. Fire safety
57. Sanitary rules 2.2.1 / 2.1.1.1278–03. Hygienic requirements for natural, artificial and combined lighting of residential and public buildings.
58. Sanitary rules 2.2.4 / 2.1.8.562–96. Noise at workplaces, in premises of residential, public buildings and in the construction area.
59. Sanitary rules 2.2.4.548–96. Hygienic requirements for the microclimate of industrial premises.
60. Sanitary rules GOST 12.1.03882 SSBT. Electrical safety. Maximum permissible levels of touch voltages and currents.
61. SanPiN 1.2.3685-21 "Hygienic standards and requirements for ensuring the safety and (or) harmlessness of environmental factors for humans"
62. SanPiN 2.2.4.3359-16 "Sanitary and epidemiological requirements for physical factors in the workplace"
63. “SN 245-71” Sanitary standards for the design of industrial enterprises”
64. “СП 52.13330.2016 Естественное и искусственное освещение. Актуализированная редакция СНиП 23-05-95* (с Изменениями N 1, 2) от 07 ноября 2016 - docs.cntd.ru.” https://docs.cntd.ru/document/456054197 (accessed May 17, 2022).